

Tertiary deformation history of southeastern and southwestern Tibet during the Indo-Asian collision

An Yin*

T. Mark Harrison

M. A. Murphy

M. Grove

S. Nie†

*Department of Earth and Space Sciences and Institute of Geophysics and Planetary Physics,
University of California, Los Angeles, California 90095-1567*

F. J. Ryerson

*Institute of Geophysics and Planetary Physics, Lawrence Livermore National Laboratory,
Livermore, California 94550*

Wang Xiao Feng

Chen Zeng Le

Institute of Geomechanics, Chinese Academy of Geological Sciences, Beijing, China

ABSTRACT

Geologic mapping and geochronological analysis in southwest (Kailas area) and southeast (Zedong area) Tibet reveal two major episodes of Tertiary crustal shortening along the classic Indus-Tsangpo suture in the Yalu River valley. The older event occurred between ca. 30 and 24 Ma during movement along the north-dipping Gangdese thrust. The development of this thrust caused extensive denudation of the Gangdese batholith in its hanging wall and underthrusting of the Xigaze forearc strata in its footwall. Examination of timing of major tectonic events in central Asia suggests that the initiation of the Gangdese thrust was approximately coeval with the late Oligocene initiation and development of north-south shortening in the eastern Kunlun Shan of northern Tibet, the Nan Shan at the northeastern end of the Altyn Tagh fault, the western Kunlun Shan at the southwestern end of the Altyn Tagh fault, and finally the Tian Shan (north of the Tarim basin). Such regionally synchronous initiation of crustal shortening in and around the plateau may have been related to changes in convergence rate and direction between the Eurasian plate and the Indian and Pacific plates. The younger thrusting event along the Yalu River valley occurred between 19 and 10 Ma along the south-dipping Great Counter thrust system, equivalent to the locally named Renbu-Zedong thrust in southeastern Tibet, the Backthrust system in south-central Tibet, and the South Kailas thrust in southwest Tibet. The coeval development of the Great Counter thrust and the North Himalayan granite-gneiss dome belt is consistent with their development being related to thermal weakening of the north Himalayan and south Tibetan crust, due perhaps to thermal relaxation of an already thickened crust created by the early phase of collision between India and Asia or frictional heating along major thrusts, such as the Main Central thrust, beneath the Himalaya.

INTRODUCTION

Intracontinental deformation resulting from the Cenozoic Indo-Asian collision (Fig. 1) is manifested by both crustal- and lithosphere-scale faulting (Peltzer and Tapponnier, 1988; Burchfiel et al., 1989, 1992; Yin et al., 1994; Leloup et al., 1995; Harrison et al., 1996; Wang and Burchfiel, 1997) and a variety of associated geologic processes, including intracontinental and continental-margin basin formation (Allen et al., 1991; Briais et al., 1993), volcanism (Deng, 1978; Coulon et al., 1986; Arnaud et al., 1992; Turner et al., 1993; Chung et al., 1998), anatexis (Le Fort, 1981; Deniel et al., 1987; Harrison et al., 1995, 1997a; Searle et al., 1997a), and concomitant metamorphism (Treloar et al., 1989; Pognante, 1993; Hodges et al., 1994; Macfarlane, 1995; Harrison et al., 1997b; Searle, 1996a). Since the publication of the landmark papers of Molnar and Tapponnier (1975) and Tapponnier and Molnar (1977) on the Cenozoic Indo-Asian collision, efforts have been focused upon determining the spatial and temporal distribution of the resulting deformation. It has been variably proposed that Cenozoic deformation in Asia has been dominated by lithospheric thickening (England and Houseman, 1986), lateral extrusion (Tapponnier et al., 1982; Peltzer and Tapponnier, 1988), continental subduction (Argand, 1924; Powell and Conaghan, 1973; Willett and Beaumont, 1994; Jin et al., 1996; Owens and Zandt, 1997), and lower-crustal channel flow (Zhao and Morgan, 1985; Bird, 1991; Avouac and Burov, 1996; Royden et al., 1997).

In general, the contrasting hypotheses cited above make specific predictions regarding the timing, style, rate, and magnitude of deformation that can only be tested by integrated geologic, geochemical, and geophysical investigations. Within this context, it is of fundamental interest to examine the kinematic evolution of the classic Indus-Tsangpo suture formed between rocks of Indian and Asian affinities throughout the collision (denoted by Great Counter thrust system in Fig. 1). Previous investigations have indicated that the precollisional magmatic-arc rocks along the southern Asian margin in the north are separated from the Paleozoic-Mesozoic sedimentary strata on the Indian shelf in the south along a boundary that underwent repeated contractional deformation. The deformation is characterized by reversal of vergence from south-directed to north-directed thrusting during late Oligocene and Miocene time (Yu and Zheng, 1979; Allègre, 1984;

*E-mail: yin@ess.ucla.edu.

†Present address: China Activity Division, Petroconsultants, P.O. Box 152, 24 Chemin de la Mairie, 1258 Perly-Geneva, Switzerland.

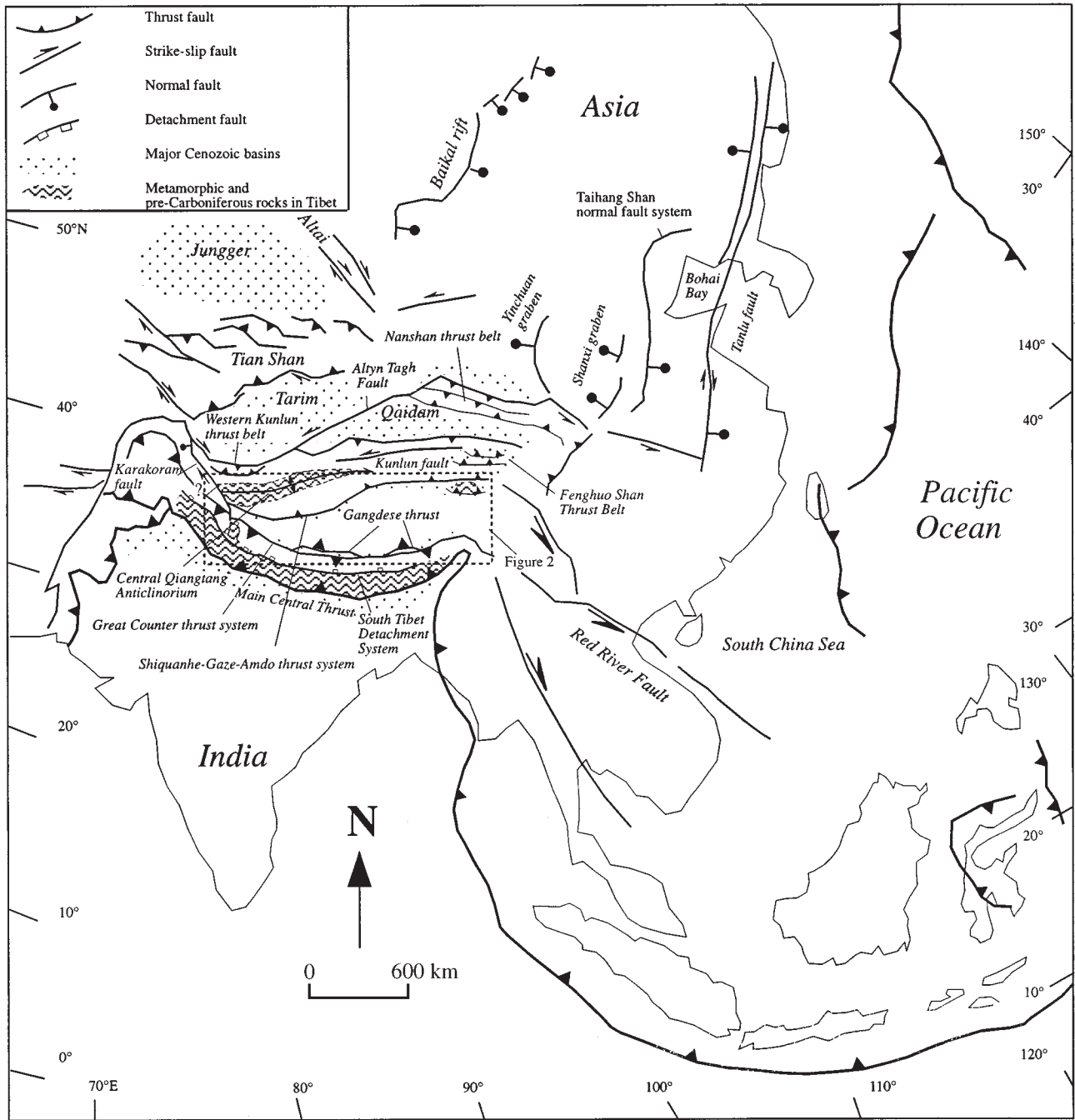


Figure 1. Cenozoic tectonic map of the Indo-Asian collisional system and location of Figure 2.

Girardeau et al., 1984; Burg, 1983; Burg and Chen, 1984; Burg et al., 1987; Searle et al., 1987; Harrison et al., 1992; Ratschbacher et al., 1992, 1994; Yin et al., 1994; Quidelleur et al., 1997). Movement on these faults appears to have overlapped in time with that of long-recognized major thrusts in the Himalayas (e.g., the Main Central thrust; Fig. 1). A recent deep-crustal seismic reflection profile across the southernmost part of Tibet reveals (1) the presence of the Main Himalayan thrust at about 40 km depth beneath the Tethyan Himalaya, which forms the sole fault for major Himalayan thrusts (Zhao et al., 1993; Nelson et al., 1996), and (2) the north-dipping South Tibetan detachment system (Burg and Chen, 1984; Burg et al., 1987; Burchfiel et al., 1992; cf. Pecher, 1991), which appears to flatten at a depth of

about 22 km, ~15–20 km above the Main Himalayan thrust (Makovsky et al., 1996; Hauck et al., 1998). However, although the integration of recent surface geologic investigations and subsurface geophysical surveys has provided a coherent geometric framework of the Himalayan orogen and its immediate northern extension in south Tibet (e.g., Owens and Zandt, 1997), key questions remain unanswered regarding the evolution of the suture between India and Asia. Specifically, why was south-directed thrusting initiated along the collision front ~20–25 m.y. after initial impingement of continental crust had taken place during the early Eocene (Patriat and Achache, 1984; Gaetani and Garzanti, 1991; Le Fort, 1996). Moreover, what triggered subsequent north-directed thrusting along this zone during the

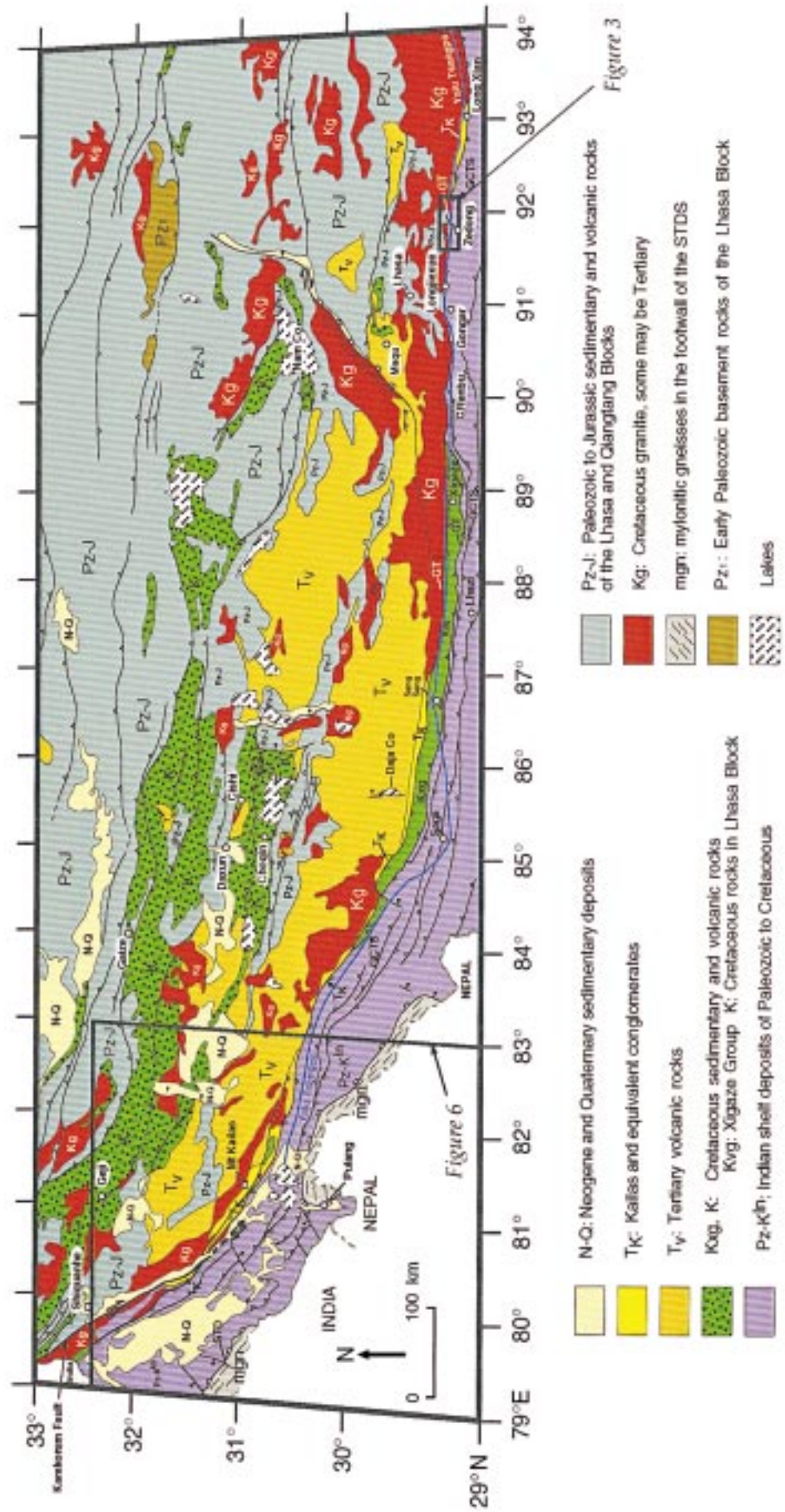


Figure 2. Simplified geologic map of southern Tibet, modified from TBGM-R (1982) with our own observations and interpretations added. Locations of Figures 3 and 6 are also shown.

Miocene and how did the reversal in vergence relate to concurrent deformation in the adjacent Himalaya?

In order to unravel the spatial and temporal evolution of the Indo-Asian collision zone, we conducted geologic investigations in the southeastern (Zedong) and southwestern (Kailas) areas of Tibet (Fig. 2). Although both locations are situated along the traditionally defined Indus-Tsangpo suture zone (Chang and Zheng, 1973; Allègre et al., 1984), the regional geologic map of the Tibetan Plateau (Liu, 1988) and our own geologic observations show that tectonic elements characteristic of suture zones (e.g., forearc basins, melanges, ophiolitic fragments, etc.) are generally missing at most locations. For example, the absence of the Xigaze forearc strata in southeast Tibet prompted investigations that ultimately led to the discovery of the Oligocene-Miocene Gangdese thrust in the Zedong area of southeastern Tibet (Harrison et al., 1992; Yin et al., 1994). Since that reconnaissance study, extensive field mapping and geochronological analyses have been conducted in the Zedong and Lang Xian areas (Fig. 2). This investigation also led to constraints upon the timing of the Renbu-Zedong thrust system. Specifically, thrust activity was found to have occurred between 19 and 10 Ma in the Lang Xian region of southeastern Tibet (Quidelleur et al., 1997; Fig. 2). To determine whether the Gangdese and the Renbu-Zedong thrusts are regionally extensive along the Indus-Tsangpo suture, we also conducted mapping and thermochronological analyses in the Kailas area of southwestern Tibet (Fig. 2).

This paper describes geologic relationships and lithologic units of the two study areas based on field mapping at a scale of 1:100 000 (Fig. 2) and presents reconnaissance-level thermochronologic measurements for the Kailas region. By coupling field mapping with thermochronological data from both this and a companion study (i.e., Harrison et al., 1999), structures in the Kailas and Zedong areas can be reasonably correlated. In particular, our fieldwork and a regional synthesis of existing geologic maps suggests the existence of a laterally continuous, south-dipping thrust system along the Indus and Yalu River valleys in southern Tibet. As the length of this thrust system is similar to that of the Main Central thrust (Fig. 1), its formation is interpreted to mark a major stage of Himalayan evolution. Because the thrust belt has a thin-skinned style and appears to have developed synchronously with the North Himalayan granite belt (Schärer et al., 1986), we speculate that its development may have been caused by thermal weakening beneath the Tethyan Himalaya that allowed southward subduction of the north Himalayan and south Tibetan basement.

GEOLOGIC MAPPING IN SOUTHERN TIBET

Southeast Tibet (Zedong Area)

Modern geologic mapping and stratigraphic investigations in southeastern Tibet date from the early 1950s (see Yu and Zheng, 1979, for references). Between 1975 and 1978, Chinese geologists participated in a systematic mapping project in the Lhasa-Zedong area (lat 28°–30°N, long 90°–96°E) that established the general stratigraphic and structural framework in this region (Yu and Zheng, 1979) and culminated in the publication of the 1:1 000 000 scale Geologic Map of the Lhasa Region. For example, the Renbu-Zedong thrust of Yin et al. (1994) or the Backthrust system of Girardeau et al. (1984), Burg and Chen (1984), and Ratschbacher et al. (1992) was first documented on this geologic map and later extended westward to the Xigaze and Kailas regions (Wang et al., 1983; Cheng and Xu, 1987). This fault was variously named the Yalu Tsangpo fault (Yu and Zheng, 1979), or the Great Yalu Tsangpo deep fault zone (Wang et al., 1983) in south-central Tibet, reflecting its general trend along the Yalu River valley. It has also been called the South Kailas thrust (Cheng and Xu, 1987) in southwest Tibet because of its excellent exposure south of Mount Kailas. Subsequently, the Sino-French (e.g., Allègre et al., 1984) and Royal Society–Academia Sinica expeditions

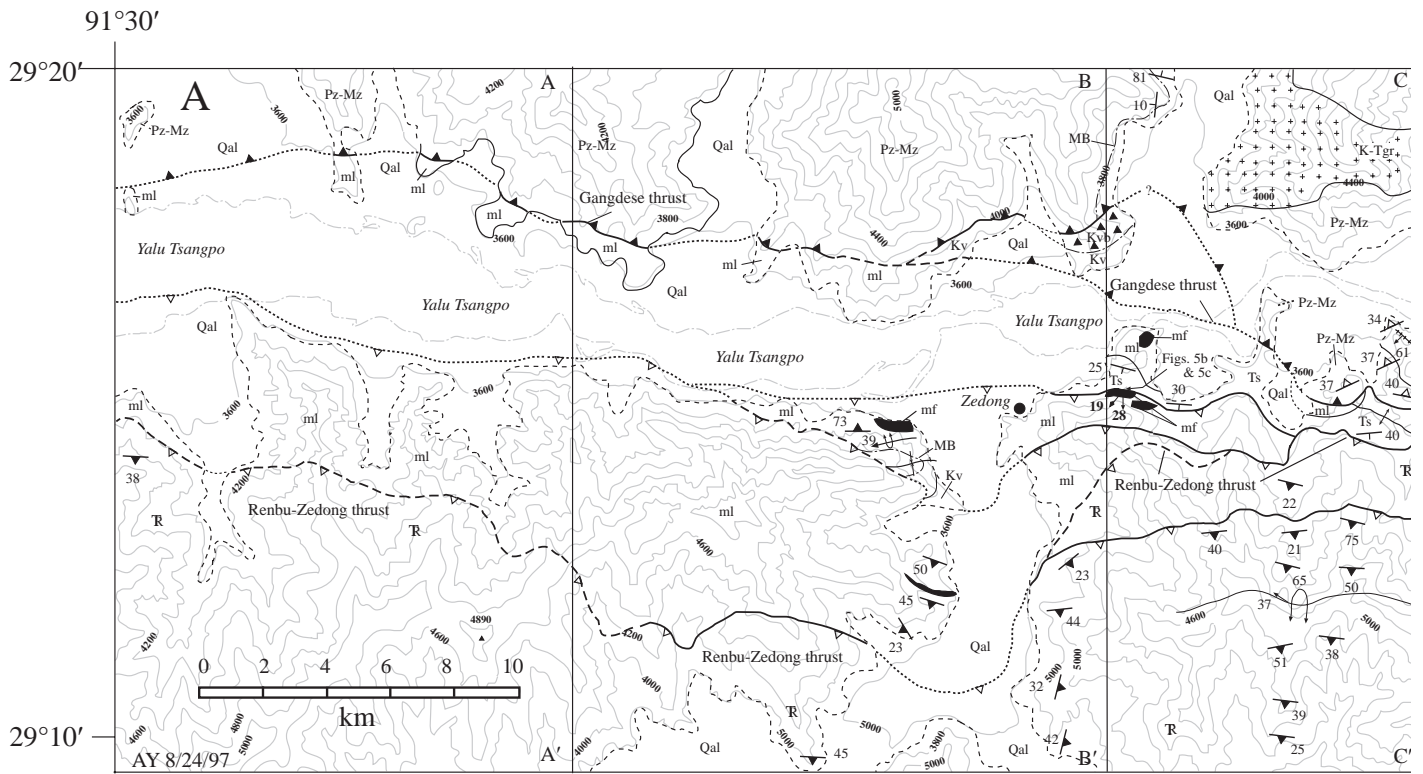
(e.g., Chang et al., 1986) resulted in a new series of regional geologic maps for south-central and central Tibet (Burg, 1983; Kidd et al., 1988). However, these international expeditions did not examine the Zedong area in detail, and thus the existence of the Gangdese thrust was not documented during these investigations. The contact between the Gangdese batholith and Tertiary conglomerates shown on the map of Yu and Zheng (1979), and the subsequently published regional map of the Tibetan Plateau (Liu, 1988), was characterized as an unconformity with Tertiary conglomerates atop the Cretaceous-Tertiary Gangdese batholith. This contact was later recognized as a north-dipping thrust, juxtaposing Gangdese igneous rocks over Tertiary conglomerates (Yin et al., 1994).

Our mapping (Fig. 3) builds upon the earlier work of Yu and Zheng (1979) and Yin et al. (1994). The latter study focused on documenting the style and timing of the Gangdese thrust motion and was restricted to a relatively small region. Subsequent, more extensive field mapping, conducted at a scale of 1:100 000 and documented in the present study, provides improved spatial coverage of the Gangdese thrust and the adjacent younger Renbu-Zedong thrust (Figs. 3 and 4). The north-dipping Gangdese and south-dipping Renbu-Zedong thrusts divide the study area into three structural domains (Fig. 3): the Gangdese hanging wall in the north, the Renbu-Zedong hanging wall in the south, and the footwall shared by both faults.

Gangdese Thrust. The hanging wall of the Gangdese thrust consists of Cretaceous-Tertiary granitoids (K-Tgr) of the Gangdese batholith, a sequence of Paleozoic and Mesozoic metasedimentary rocks (Pz-Mz), Cretaceous volcanic and interbedded clastic strata (Kvb and Kv), and a gneiss complex (mgn) (Fig. 3). The metasedimentary rocks (Pz-Mz) above the Gangdese thrust (Fig. 3) are mainly marble, phyllite, and schist with strong stretching lineations near the Gangdese thrust. The metasedimentary sequence (Pz-Mz in Fig. 3) had been assigned to the Early Cretaceous on the basis of a regional lithologic correlation (Yu and Zheng, 1979), although no fossils have been found in these rocks. The fact that these rocks can equally well be correlated with other Paleozoic and Mesozoic units in the region leads us to assign them a much broader range of ages. The volcanic flow and breccia units (Kv and Kvb in Fig. 3) consist of andesite, interbedded quartz arenite, shale, pyroclastic breccias, and siltstone. The volcanic units are correlated with the Lower Cretaceous Linbuzhong Formation by Yu and Zheng (1979). Near the Gangdese thrust, plagioclase phenocrysts in the andesites are highly stretched and aligned uniformly in the direction parallel to the regional stretching lineation in the mylonitic shear zone directly above the Gangdese thrust.

A coarse-grained biotite-hornblende gneiss (mgn) of unknown age and affinity is present as a tectonic sliver between two thrusts in the Gangdese thrust fault zone (Fig. 3). The schistosity defined by coarse biotite and flattened quartz grains within the gneiss is unlike fabrics exhibited by finer-grained wall rocks within the hanging wall of the Gangdese thrust and instead resembles that of the Amdo gneiss situated ~350 km north of Lhasa (Liu, 1988; Kidd et al., 1988). Stretching lineations in the gneiss trend N80°E, which is nearly perpendicular to the general trend of mylonitic lineations in the shear zone of the Gangdese thrust (Fig. 3).

Above the thrust, the relative proportion of granitoid (K-Tgr in Fig. 3) to wall rock (Pz-Mz in Fig. 3) increases eastward. This eastward increase in the exposure area of plutonic rocks correlates with progressively higher metamorphic grades in the Tethyan metasedimentary rocks as the eastern syntaxis is approached (Fig. 2; Liu, 1988; Quidelleur et al., 1997). The plutonic bodies in the Zedong region are generally tabular in shape and parallel to relict bedding and foliation in the hanging wall of the Gangdese thrust (Fig. 3). Foliation is, in general, subparallel to the Gangdese thrust. The near-concordance of fabric elements (relict bedding, foliation, tabular plutonic bodies) with the Gangdese thrust is consistent with the interpretation that the present exposure of the steeply dipping Gangdese thrust sheet (Fig. 4) likely originated along a subhorizontal detachment. The inferred geometry is consistent



MAP LEGEND

Qal	Quaternary alluvial deposits	K-Tgr	Cretaceous to Tertiary granodiorites of the Gangdese batholith
Tc	Tertiary conglomerate (=Luobusha Group)	syn	Late Cretaceous to early Tertiary syenite
Kv	Andesitic flow and tuff of possibly Cretaceous age	mf	Mafic and ultramafic bodies in the melange
Kvb	Andesitic flow and breccias of possibly Cretaceous age	ml	Melange complex including cherty units, shale, marble, andesite, diorite, mafic and ultramafic bodies, limestone, and phyllite. Limestone units contain Late Cretaceous fossils.
R	Late Triassic Longjiexue Group, mostly fine-grained sandstone and phyllite	mgn	Mylonitic gneisses
Pz-Mz	Undifferentiated Paleozoic and Mesozoic strata, Mostly sandstone, shale, interbedded with andesite		

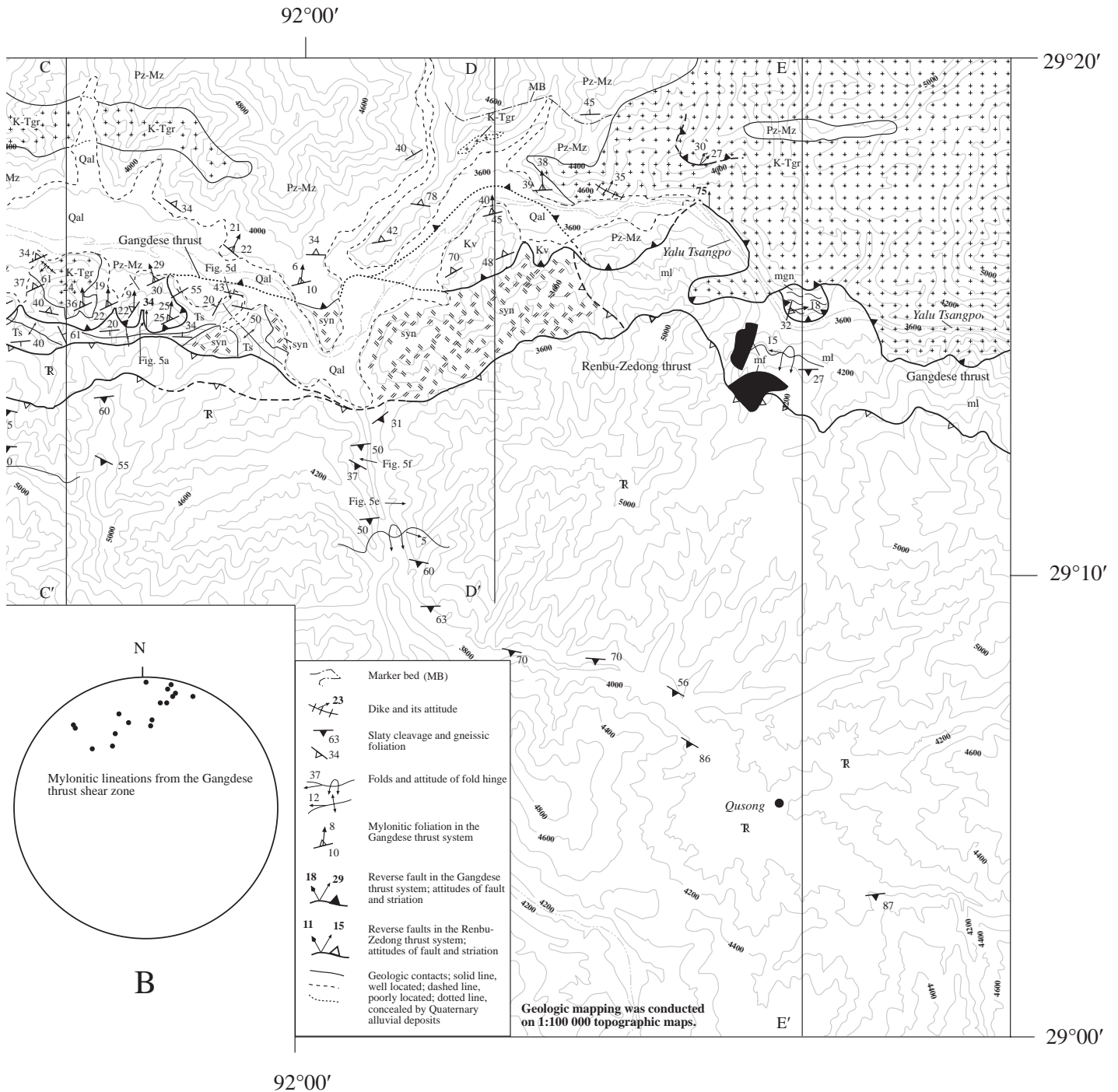
Figure 3. (A) Geologic map of the Zedong area and locations of field pictures shown in Figure 5. Qal—Quaternary alluvial deposits; Ts—Tertiary conglomerate; Kv and Kvb—Cretaceous andesites and volcanic breccias; ml—melange complex; K-Tgr—Cretaceous to early Tertiary granites; syn—syenite, possibly Cretaceous in age; Pz-Mz—Paleozoic to Mesozoic sedimentary and metasedimentary rocks in the hanging wall of the Gangdese thrust; mgn—gneissic complex of unknown age; mf—mafic and ultramafic bodies; Tr—Triassic strata in the hanging wall of the Renbu-Zedong thrust. See Figure 2 for location. (B) Stereographic projection of stretching lineations measured in the mylonitic shear zone of the Gangdese thrust. Majority of the lineations trend between N20°W and N20°E.

with a systematically decreased depth of exposure of the Gangdese batholith north of our study area (Fig. 2; Liu, 1988; Copeland et al., 1995).

The main trace of the Gangdese thrust system is well exposed in several places along the Yalu River (Figs. 3 and 5A). In most places, the Gangdese thrust is marked by an ~50–150-m-thick mylonitic shear zone consisting of marble, granitoid, and schist. Mesoscopic asymmetric folds, asymmetric boudinage, minor reverse faults, and S-C fabrics in the mylonitic granitoids all indicate a top-to-the-south sense of shear (Yin et al., 1994). Foliations are well developed, and the general trend of lineations is between S20°W and

S20°E (Fig. 3). The dip angle of the fault varies considerably from 34° in the central part of the study area to 75° in the east (Fig. 3). The abrupt change in the strike and dip angle of the Gangdese thrust (east of D–D'; Fig. 3) reflects postslip deformation of the fault surface.

Renbu-Zedong Thrust. The south-dipping Renbu-Zedong thrust in the Zedong region, and its western extension, is the dominant structural element of the suture zone (Heim and Gansser, 1939; Burg, 1983; Thakur and Sharma, 1983; Yin et al., 1994; Ratschbacher et al., 1992, 1994; Quidelleur et al., 1997; Searle et al., 1997b). Near Zedong, this fault juxtaposes an iso-



clinally folded sequence of shale, siltstone, phyllite, and locally schist over the melange, syenites, and Tertiary conglomerate. On the basis of fossils described in similar strata (Yu and Zheng, 1979; Table 1) about 100 km west of our study area, we conclude that the Tethyan strata we have examined are likely Late Triassic in age. Finally we emphasize that east of the mapped area, the hanging wall of the Renbu-Zedong fault is thrust over the trace of the Gangdese thrust, clearly indicating that the former is a younger feature (Yin et al., 1994; Fig. 2).

Isoclinal folding of the Tethyan strata in the Renbu-Zedong hanging wall (Fig. 5B) is associated with pervasive slaty cleavage that consistently dips

south. Top-to-the-north, noncoaxial shear deformation is evident in the folded rocks. For example, the orientation of ubiquitous en echelon quartz veins suggests top-to-the-north shearing (Fig. 5C). Because these vein sets are further deformed (faulted and folded) in a manner consistent with the same sense of shear (Fig. 5C), protracted shear deformation is indicated. The association of vein quartz with axial cleavage suggest that simple-shear deformation and isoclinal folding were synchronous and likely related. We interpret that isoclinal folding and north-directed noncoaxial deformation in the folded rocks were related to Tertiary northward movement along the Renbu-Zedong thrust. This interpretation is consistent with K/Ar dating of

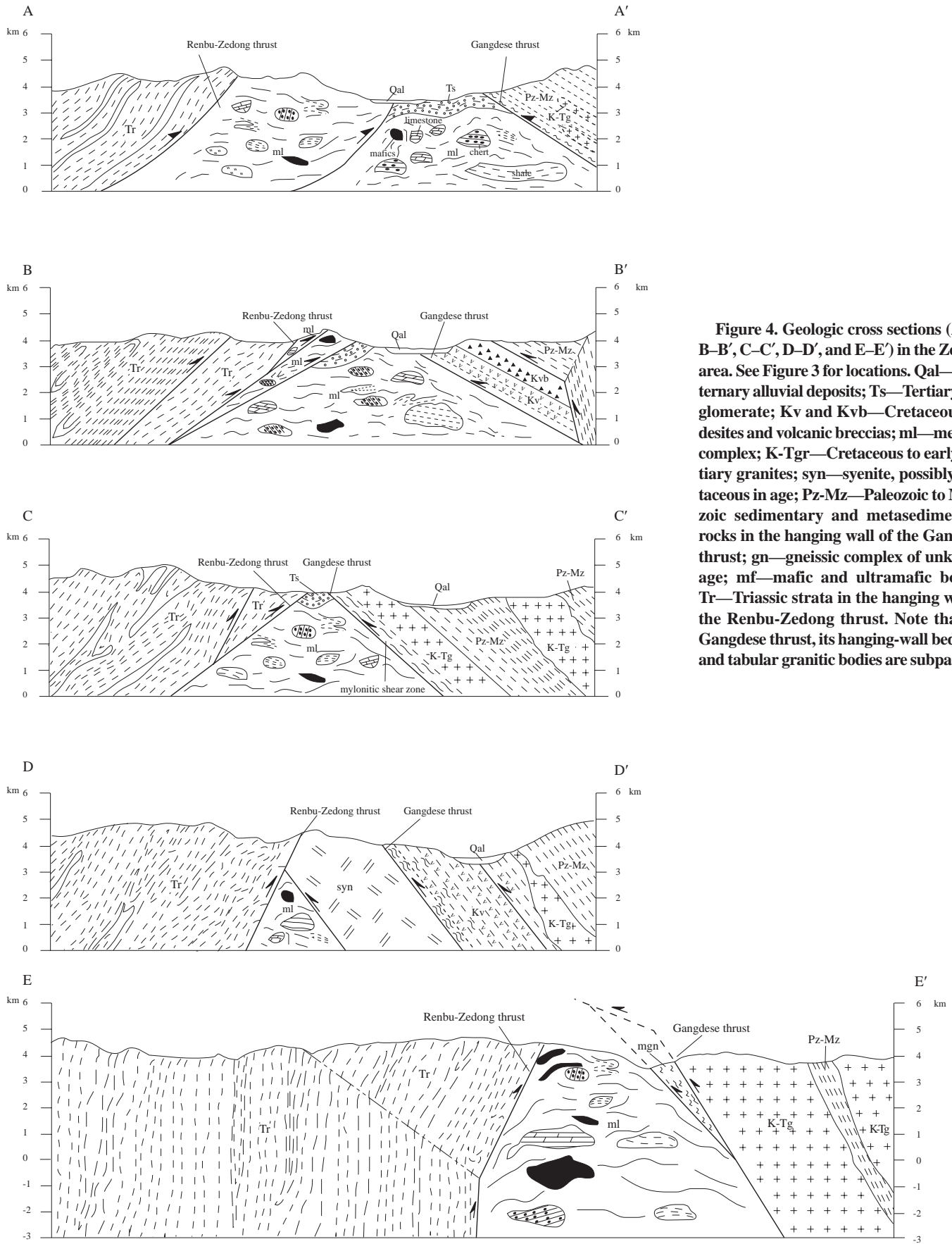


Figure 4. Geologic cross sections (A-A', B-B', C-C', D-D', and E-E') in the Zedong area. See Figure 3 for locations. Qal—Quaternary alluvial deposits; Ts—Tertiary conglomerate; Kv and Kvb—Cretaceous andesites and volcanic breccias; ml—melange complex; K-Tgr—Cretaceous to early Tertiary granites; syn—syenite, possibly Cretaceous in age; Pz-Mz—Paleozoic to Mesozoic sedimentary and metasedimentary rocks in the hanging wall of the Gangdese thrust; gn—gneissic complex of unknown age; mf—mafic and ultramafic bodies; Tr—Triassic strata in the hanging wall of the Renbu-Zedong thrust. Note that the Gangdese thrust, its hanging-wall bedding, and tabular granitic bodies are subparallel.

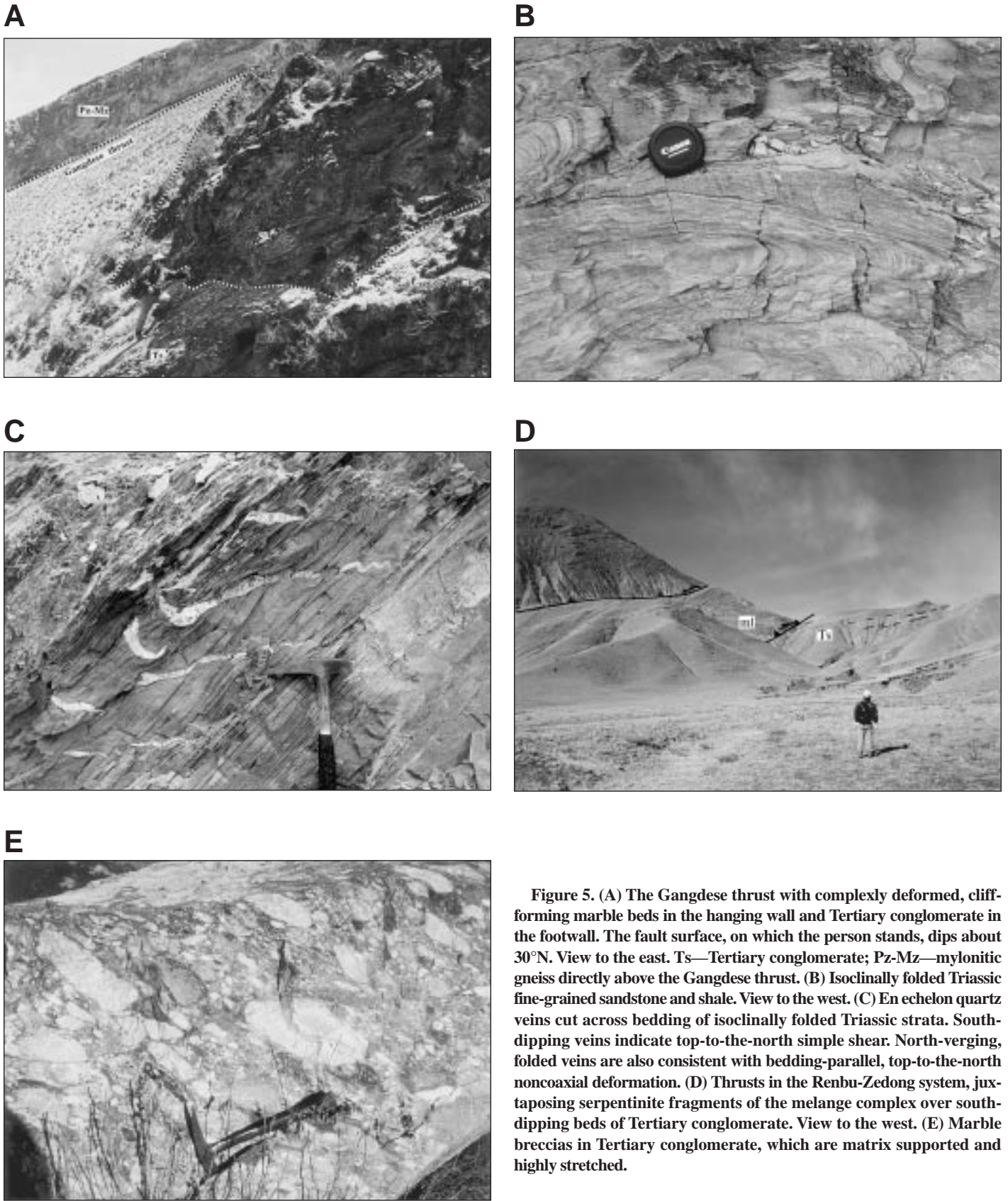


Figure 5. (A) The Gangdese thrust with complexly deformed, cliff-forming marble beds in the hanging wall and Tertiary conglomerate in the footwall. The fault surface, on which the person stands, dips about 30°N. View to the east. Ts—Tertiary conglomerate; Pz-Mz—mylonitic gneiss directly above the Gangdese thrust. (B) Isoclinally folded Triassic fine-grained sandstone and shale. View to the west. (C) En echelon quartz veins cut across bedding of isoclinally folded Triassic strata. South-dipping veins indicate top-to-the-north simple shear. North-verging, folded veins are also consistent with bedding-parallel, top-to-the-north noncoaxial deformation. (D) Thrusts in the Renbu-Zedong system, juxtaposing serpentinite fragments of the melange complex over south-dipping beds of Tertiary conglomerate. View to the west. (E) Marble breccias in Tertiary conglomerate, which are matrix supported and highly stretched.

TABLE 1. PALEONTOLOGIC AGE CONSTRAINTS FROM FOSSILIFEROUS STRATA

Map unit	Probable depositional age	Fauna and flora reported
Chert melange (near Zedong)	Late Cretaceous*	Foraminifera: <i>Orbitolina concava</i> (Lamarck), <i>O. sp. cf. O. lamina</i> Ho, <i>O. aperta</i> (Erman), <i>O. sp. cf. O. conica</i> (Dinrchiac) Corallina: <i>Thamnasteria sp. cf. T. matsushitai</i> Eguchi
Luobusha Group (near Zedong)	Oligocene(?)* (possibly Eocene–Miocene)	Gastropods: <i>Planorbis sp. cf. P. rotundata</i> Brong, <i>Bithynia sp.</i> , <i>Lymnaea sp.</i> , <i>Microlaminatus sp.</i> , <i>Planorbarius sp.</i> , <i>Gyraulus sp.</i> , <i>Fluminicola sp.</i> , <i>Amnicola sp.</i> Bivalves: <i>Sphaerium sp. aff. S. rivicolam</i> Lamarck, <i>Acuticosta sp.</i> Algae: Charophyta gen. et sp. indet., <i>Tectochara sp.</i> , <i>Crofiella sp.</i> Plant fossils: <i>Palmocarpon sp.</i> , <i>Rhododendron sp.</i>
Himalayan Tethyan metasediments (near Longjiexue)	Late Triassic*	Bivalves: <i>Halobia vietnamica</i> Vukhus, <i>H. sp. cf. H. yunnanensis</i> Keed, <i>H. sp. cf. H. ganzhiensis</i> Chen, <i>H. sp. aff. H. styriaca</i> Mojs., <i>H. sp. cf. H. xizangensis</i> Wen et Lan, <i>H. sp. cf. H. cordillerana</i> Smoth, <i>H. sp. cf. H. comata</i> Bittner, <i>H. sp. cf. H. austyriaca</i> Mojs., <i>H. sp. cf. H. plicosa</i> Mojs., <i>Manticula ? sp.</i> , <i>Posidonia sp. aff. P. wegensis</i> Wissm. Brachiopods: <i>Koninckina sp.</i>
Yiema Formation (in the Kailas area)	Cretaceous†	Gastropods: <i>Nerinea sp. cf. N. pauli</i> Coquand Bivalves: Radiolittidae gen. et sp. indet.

*Data source: Yu and Zheng (1979).

†Data source: Cheng and Xu (1987).

white mica from a synkinematic mica-bearing quartz vein in the Renbu-Zedong fault zone near Renbu (Fig. 2); the white mica yielded an age of ca. 18 Ma (Ratschbacher et al., 1994).

The Renbu-Zedong fault zone consists of several imbricate thrusts in both its footwall and hanging wall. Although the latter can be well located in the field, the main trace of the Renbu-Zedong thrust itself is mostly covered by talus in the mapped area. However, minor thrusts that juxtapose the melange complex over Tertiary conglomerate is well exposed about 3 km east of Zedong (Figs. 2 and 5D). At this locality, a highly sheared serpentinite block is present in the hanging wall of a fault branch in the Renbu-Zedong thrust system. The fault dips 28°S with striations trending to the southwest (Fig. 3). Kinematic indicators (e.g., en echelon tension gashes, asymmetric folds, etc.) in the rocks a few meters above and below the fault show a consistent top-to-the-north sense of shear. In general, the dip angle of the cleavage in the Triassic strata increases southward, from about 20–30° directly above the Renbu-Zedong thrust to nearly vertical, 15–20 km south of the fault trace (Fig. 3). Such a systematic change in cleavage dip may reflect a change in the geometry of the Renbu-Zedong thrust at depth (see cross section E–E' in Fig. 4). An equally plausible interpretation of the variation in cleavage orientation in the hanging wall of the thrust would be that the cleavage becomes progressively steeper toward higher structural levels in the hanging wall. Such a listric geometry is common in many mountain belts in the world (e.g., Mitra, 1994).

A key to testing the two alternative explanations is to detect whether bedding changes systematically, as it would if cleavage and hanging-wall strata rotate passively as the thrust sheet moves across a steep footwall ramp. However, the folds in the study area above the Renbu-Zedong thrust are isoclinal (Fig. 5B). Thus, the bedding and cleavage are nearly parallel in general except near the fold hinges, making it difficult to select between the two possible structural interpretations.

Footwall of Gangdese and Renbu-Zedong Thrusts. Rocks exposed in the footwall of the opposing thrusts include chert-dominated melange, syenite bodies, and Tertiary conglomerates (Figs. 3 and 4). Locally, syenite is thrust over melange, whereas the conglomerate unit is deposited unconformably on top of both units. In addition to chert, the melange complex contains blocks or domains of thinly bedded and massive quartzite, shale, serpentinite, limestone, gabbros, and, locally, volcanic breccias. The serpentinite blocks are highly sheared with abundant striations and are uniquely distributed along the Renbu-Zedong fault zone. Limestone and cherty layers in the melange complex are tightly folded and refolded, with

wavelengths and amplitudes on the order of several hundreds of meters. Late Cretaceous fossils occur within elements of the melange complex near Zedong (Yu and Zheng, 1979, p. 89; see Table 1). Yu and Zheng (1979) suggested that these Upper Cretaceous rocks (Fig. 2) are correlative to the Cretaceous–Eocene Xigaze forearc strata farther to the west in the Xigaze area (Fig. 1), which include both the middle to Upper Cretaceous Xigaze Group (Wang et al., 1983; Wiedmann and Durr, 1995; Durr, 1996) and the overlying lower Tertiary Quwu Formation (Wang et al., 1983). This correlation supports the interpretation of Harrison et al. (1992) that the Xigaze forearc once existed in southeastern Tibet and has been largely underthrust beneath the Gangdese batholith along the Gangdese thrust system.

Lying unconformably on top of the melange and syenites is a >200-m-thick sequence of Tertiary conglomerate referred to by Yu and Zheng (1979) as the Luobusha Group (Table 1). Fossil occurrences reported by Yu and Zheng (1979) for the Luobusha Group in the Zedong area (Table 1) suggest an Oligocene depositional age, although fossils consistent with Eocene and Miocene deposition are also present. An Oligocene age assignment is consistent with our interpretation that the deposition of the Luobusha Group was due to denudation of the Gangdese batholith and associated with thrusting along the Gangdese thrust during this time (Yin et al., 1994; Harrison et al., 1999). Cobbles and boulders within the Tertiary conglomerate, dominantly marble and volcanic breccia, are typically matrix supported. Although these clasts can be correlated with the rock units in the Gangdese thrust hanging wall, granitic clasts are rarely present in the outcrops we examined. Bedding within the conglomerate is broadly folded with east-trending fold axes (Fig. 3). Adjacent to the Gangdese thrust, clasts are strongly deformed and exhibit aspect ratios between 5:1 and 15:1 (Fig. 5E).

Southwest Tibet (Kailas Area)

Gansser first recognized a north-directed thrust that juxtaposes a flysch complex over a sequence of conglomerate in the Kailas area (Heim and Gansser, 1939). Heim and Gansser (1939) named this structure “the Great Counter thrust” to contrast it with the dominantly south-directed thrusting in the Himalaya to the south. The >2000-m-thick Kailas conglomerate (Gansser, 1964) rests unconformably on top of granitoids of the Gangdese batholith (Fig. 6).

Regional mapping of the Kailas region (lat 28°–32°N, long 78°–82°E) by the Tibetan Bureau of Geology and Mineral Resources (Cheng and Xu, 1987) extended the Great Counter thrust, renamed as the South

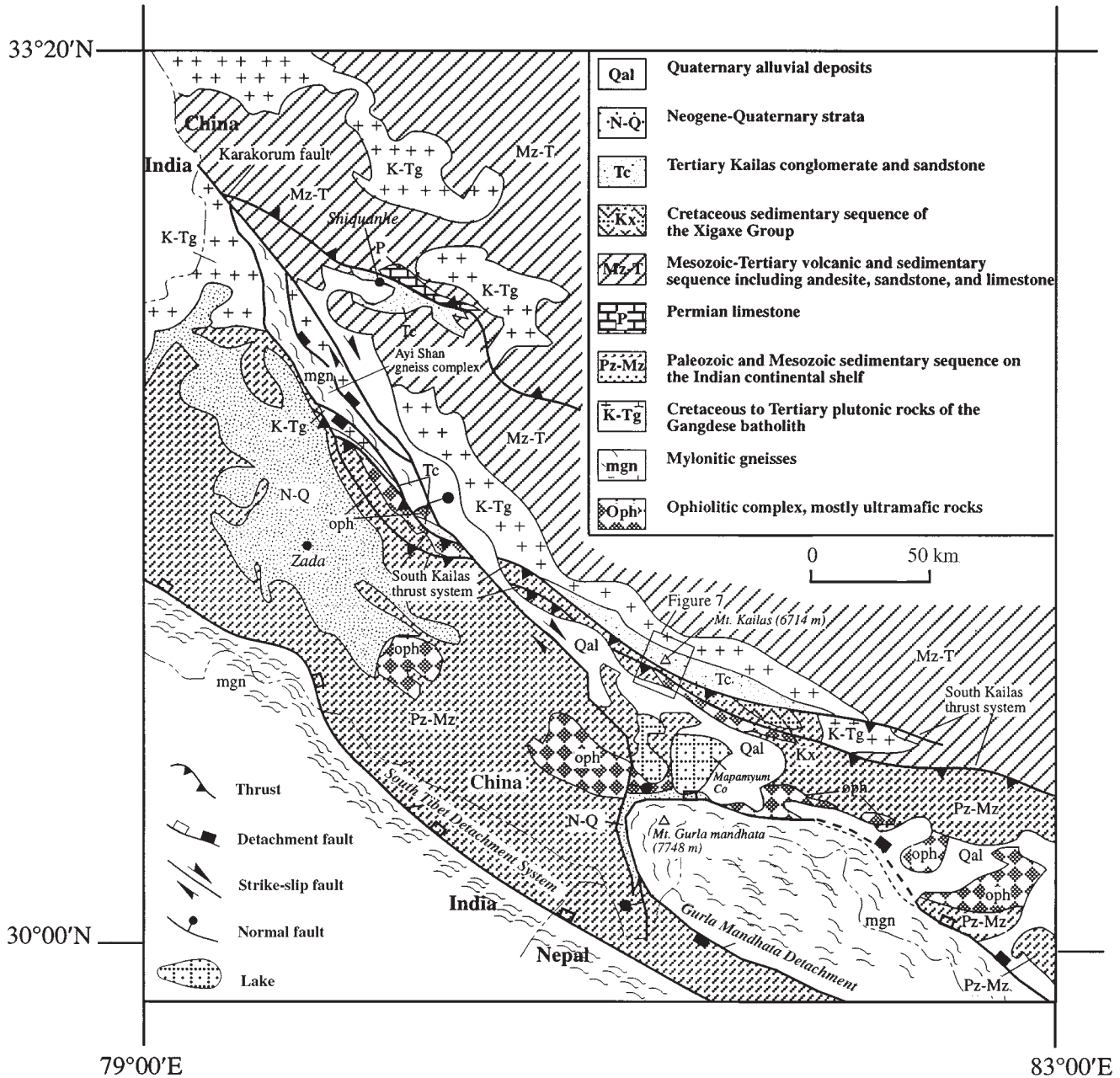


Figure 6. Geologic map of the Kailas–Gurla Mandhata region based on both our own mapping and a 1:1 000 000 geologic map of the region by Cheng and Xu (1987).

Kailas thrust, 210 km farther to the east. The South Kailas thrust was in turn linked by Liu (1988) with the “Great Yalu Tsangpo deep fault” of Wang et al. (1983) in the Xigaze area. To the west, the displaced western continuation of the South Kailas thrust across the Karakoram fault has been recognized by Murphy et al. (1997b) (Fig. 6). This correlation suggests that the post–middle Miocene dextral displacement of the Karakoram fault was <50 km at its southeastern termination. To avoid confusion, we refer to the south-dipping thrust system in the Kailas area as the South Kailas thrust system. We collectively refer to the overall south-dipping thrust system developed along the Indus and Yalu River valleys in southern Tibet (including the Backthrust system of Girardeau et al. [1984] and

Ratschbacher et al. [1992] and the Renbu-Zedong thrust of Yin et al. [1994]) as the Great Counter thrust system (Fig. 1).

South Kailas Thrust System. Rocks within the Kailas area were mapped in the summer of 1995 by A. Yin and M. Murphy at a scale of 1:100 000 (Fig. 7). The goals of this investigation were twofold: (1) to better document the geometry and kinematics of north-directed thrusting in the area and (2) to constrain the timing of thrusting of the South Kailas thrust and the timing of denudation of the Gangdese batholith. The major geologic features based on our mapping are briefly described below. The Kailas conglomerate (Heim and Gansser, 1939; Gansser, 1964) or the Kailas Formation (Cheng and Xu, 1987) rests unconformably on top of the

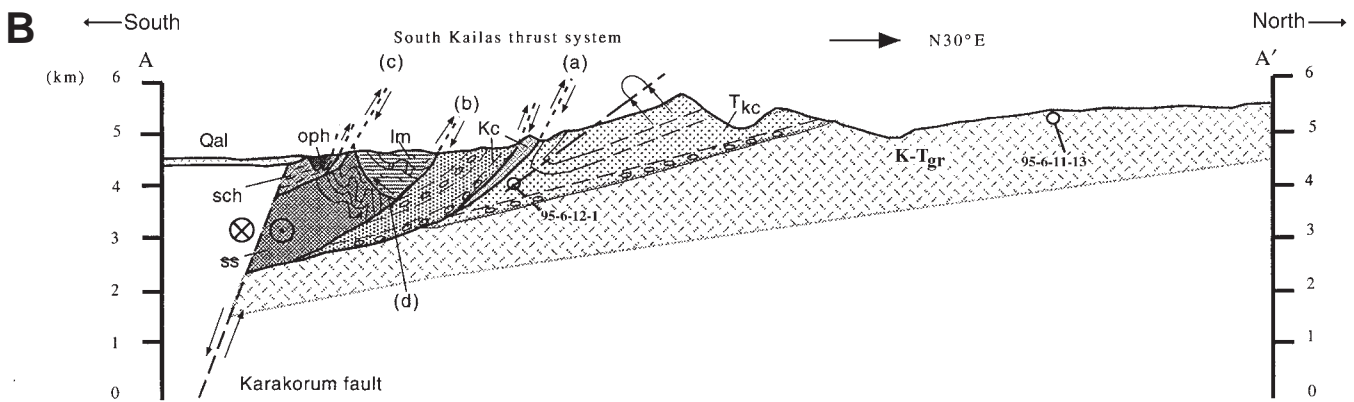
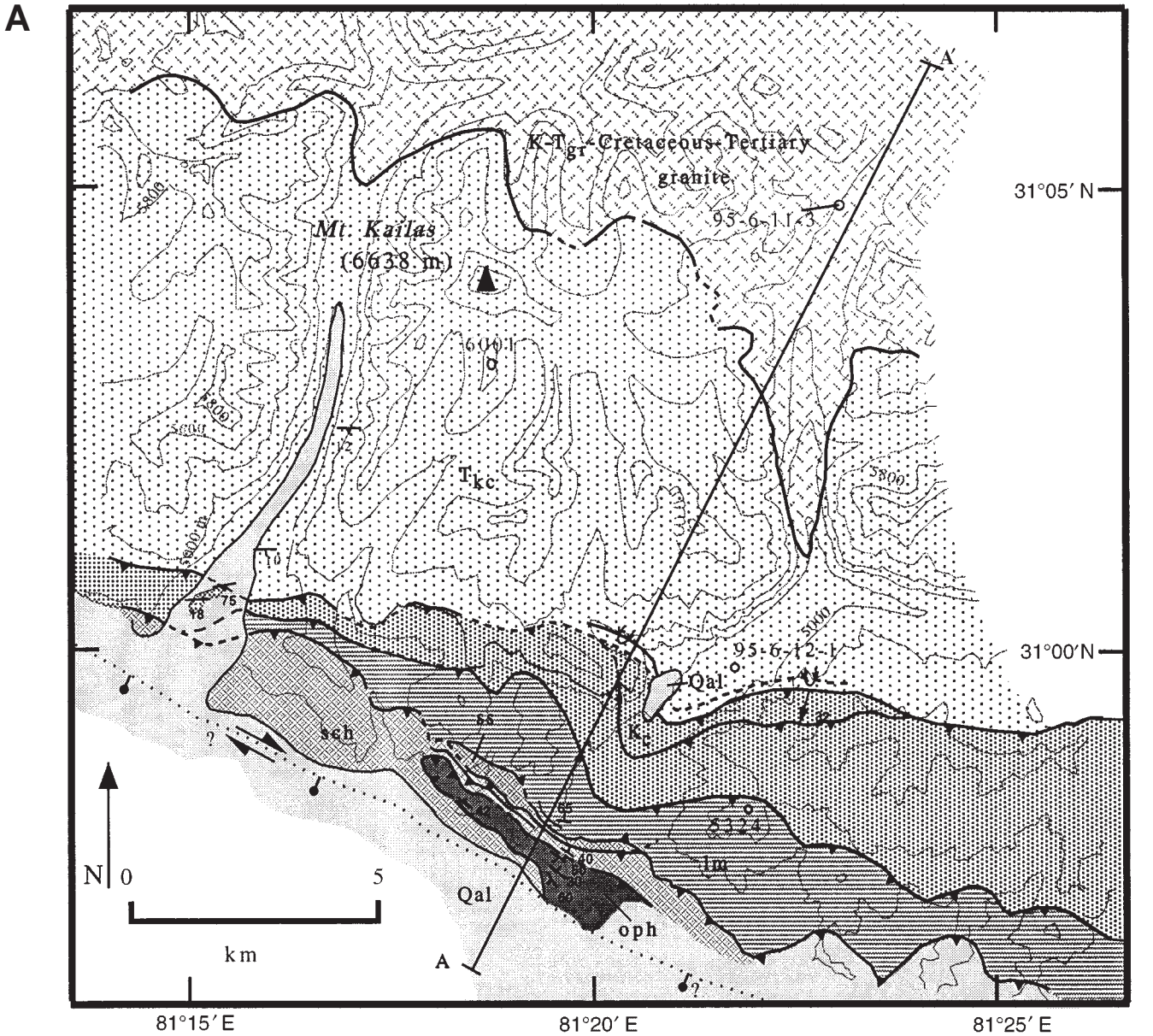


Figure 7. Geologic map (A) and cross section (B) of the Mount Kailas area. Mapping was conducted at a scale of 1:100 000. Numbers on map and cross section are sample locations. Qal—Quaternary alluvial deposits in Gar Valley; K-T_{gr}—Cretaceous–Tertiary granitoids; T_{kc}—Tertiary Kailas conglomerate; Kc—possible Cretaceous to Tertiary conglomerate and sandstone; lm—a limestone unit, possibly part of the Cretaceous Xigaze Group (Liu, 1988); sch—schist of unknown age, possibly part of the Indian continental shelf deposits; ss—sandstone unit of unknown age and origin; oph—ophiolite complex.

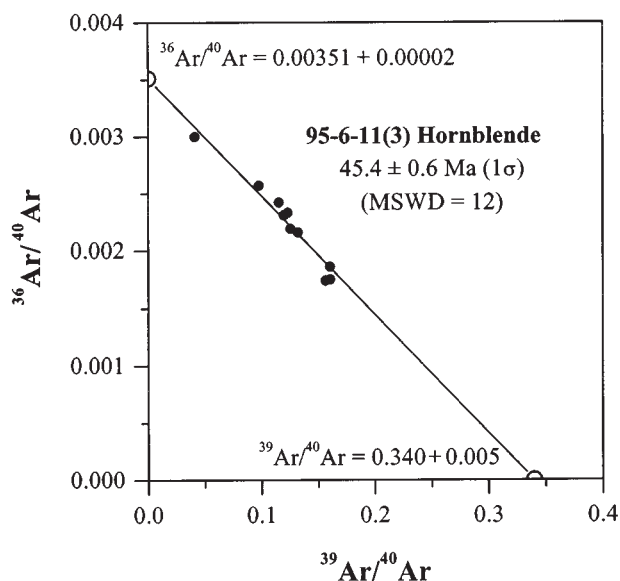


Figure 8. $^{40}\text{Ar}/^{39}\text{Ar}$ isochron for hornblende from Kailas intrusive complex, sample 95-6-11(3).

Kailas magmatic complex (Honegger et al., 1982), part of the Gangdese batholith (Fig. 2). The exposure of the Gangdese batholith in southwest Tibet is limited to the southernmost region of the Gangdese Shan. North of Mount Kailas (Fig. 2), the exposure is dominated by Late Cretaceous–early Tertiary volcanic cover, indicating a systematic decrease in the amount of denudation of the Gangdese batholith to the north (Fig. 2). The greater amount of denudation in the southern part of the Gangdese batholith in the Kailas and surrounding regions suggests oblique exposure of a tilted crustal section along the south margin of the batholith, similar to that seen in southeastern Tibet (Fig. 2).

Conglomerate beds dip a few degrees to the south immediately above the unconformity (Fig. 7). The lower part of the Kailas conglomerate, about 200–400 m thick, is dominated by granitoid and volcanic cobbles that record south-directed paleocurrents. The clasts can be directly correlated with Gangdese granites and its volcanic cover (Heim and Gansser, 1939; Honegger et al., 1982). The middle part of the formation, about 1500–2000 m thick, consists of medium- to fine-grained sandstones, which we tentatively interpret to have developed in a meandering fluvial setting. This sequence shows a generally westward paleocurrent direction, which is parallel to the trend of the South Kailas thrust. The inferred west-flowing drainage system may have been controlled by the existence of a foredeep during the northward emplacement of the South Kailas thrust system. The top part of the Kailas conglomerate, at least 300 m thick, is characterized by pebbles and cobbles of metamorphic schists, volcanic breccias, and purple and green sandstones. In contrast to the granitic clasts, which dominate the lower part of the Kailas conglomerate, these clasts are characteristic lithologies of the South Kailas thrust system and thus must have been derived from the south. The appearance of coarse clastic material deposited higher up in the Kailas conglomerate is also associated with abundant northward paleocurrent indicators (e.g., pebble imbricates), consistent with the above interpretation.

Immediately adjacent to the northernmost south-dipping thrust (fault (a) in Fig. 7B), the Kailas conglomerate (Tkc in Fig. 7) is abruptly overturned and strongly deformed (Fig. 7). This north-directed thrust was first documented by Heim and Gansser (1939). It places a sequence of distinctive conglomerate and interbedded sandstone layers (Kc in Fig. 7) atop the Kailas conglomerate. The unit was named the Yiema Formation by Cheng

and Xu (1987) and contains dominantly purple and gray sandstone, andesitic volcanic breccias, and limestone that yields Cretaceous fossils (Cheng and Xu, 1987; Table 1). The limestone and sandstone units were inferred by Liu (1988) to be part of the Cretaceous Xigaze forearc deposits. A second north-directed thrust (fault (b) in Fig. 7B) south of the frontal thrust (not documented in Heim and Gansser, 1939) places a highly folded limestone and calcareous schist unit (lm in Fig. 7) over the Cretaceous Yiema Formation (Kc in Fig. 7). The age of the limestone unit is not known, but it may be part of the Paleozoic–Mesozoic shallow-marine sedimentary sequence deposited on the northern Indian shelf prior to the Indo-Asian collision or part of the Cretaceous Xigaze forearc sequence. In any case, the depositional age of the unit likely predates the initial collision between India and Asia. This complexly deformed limestone unit exhibits well-developed south-dipping spaced cleavage in the limestone beds. Farther to the south, the limestone unit is thrust over a purple sandstone unit (ss in Fig. 7) along a north-dipping thrust (fault (d) in Fig. 7B). Both the limestone and sandstone units were underthrust beneath a north-directed thrust (fault (c) in Fig. 7B) that carries a phyllitic schist unit (sch) in its hanging wall. The hanging wall of this thrust (c) contains a shallow-dipping fault, which is folded with a northward vergence. The uppermost fault in the study area places serpentinite (oph) over both the phyllitic schist (sch), purple sandstone (ss), and locally the limestone (lm) units (Fig. 7). Both the age and transport direction of this folded thrust are unknown.

The above crosscutting relationship indicates that at least two phases of thrusting occurred in the Kailas area: the early event was south directed whereas the younger event was north directed. Although the younger thrusting is clearly Tertiary, as it cuts the Tertiary Kailas conglomerate (see discussion below), the age of the older event is not well constrained.

Age Constraints

Southeast Tibet (Zedong Area). Here, we briefly summarize the results of a detailed thermochronologic and geochronologic investigation of the Zedong area (see details in Harrison et al., in press). An upper bound for the initiation of slip along the Gangdese thrust is obtained from the crystallization age of a hanging-wall granodiorite, dated by U–Pb ion microprobe measurements on zircon at 30.4 ± 0.4 (Harrison et al., 1999). The intrusion is cut by the Gangdese thrust and is affected by the same mylonitic fabric that characterizes other hanging-wall rocks in close proximity to the fault (see Fig. 3, cross section C–C', for location). Hornblendes extracted from the same intrusion yield similar $^{40}\text{Ar}/^{39}\text{Ar}$ ages. It is interesting that emplacement of this granodiorite occurred ~10–15 m.y. after the last recognized phase of igneous activity within the Gangdese batholith (e.g., TBGMR, 1982; Schärer and Allègre, 1984; Coulon et al., 1986; Copeland et al., 1995; Pan, 1993).

Thermochronometry along traverses west of cross section E–E' in Figure 3 that vary from 0.5 to 1 km in vertical component are consistent with thrust-related cooling beginning at ca. 28 Ma and continuing until 24 Ma (Harrison et al., 1999). In contrast, K-feldspar samples positioned east of cross section E–E' exhibit broader age gradients with minimum ages as young as 8 Ma. These age systematics strongly resemble those exhibited by the Gangdese granitoids overthrust by the Renbu-Zedong thrust east of Lang Xian (Fig. 2; Quidelleur et al., 1997). For Gangdese batholith samples in the easternmost part of Figure 3, minimum K-feldspar ages decrease to the southeast. Differential tectonic loading produced by greater overthrusting of the Renbu-Zedong thrust toward the east, coupled with synthrust deformation of the Renbu-Zedong thrust footwall, may have promoted greater outgassing of eastern samples during middle Miocene to late Miocene time relative to western samples that resided at shallower depths (Harrison et al., 1999). The Gangdese thrust is buried beneath the Renbu-Zedong thrust hanging wall just west of the region mapped in Figure 3, reproducing the geologic relationship observed east of Lang Xian (Fig. 2; Quidelleur et al., 1997).

TABLE 2

Step	T (°C)	t (min)	⁴⁰ Ar/ ³⁹ Ar	³⁷ Ar/ ³⁹ Ar	³⁶ Ar/ ³⁹ Ar	³⁹ Ar (mol)	Σ ³⁹ Ar (%)	⁴⁰ Ar* (%)	Age ± 1σ (Ma)
95-6-11(3) Hornblende (J = 0.00866) Total gas age = 46.19 ± 1.17 Ma									
1	800	17	10.26	1.23	2.66 × 10 ⁻²	3.06 × 10 ⁻¹⁴	13.3	24.1	38.3 ± 0.6
2	950	21	6.207	9.31	1.31 × 10 ⁻²	4.40 × 10 ⁻¹⁴	32.4	48.3	46.5 ± 0.3
3	980	12	6.326	19.8	1.58 × 10 ⁻²	2.14 × 10 ⁻¹⁴	41.6	48.8	48.2 ± 0.7
4	1010	11	6.174	18.6	1.59 × 10 ⁻²	1.80 × 10 ⁻¹⁴	49.4	45.2	43.6 ± 0.6
5	1030	12	8.074	14.2	2.23 × 10 ⁻²	8.62 × 10 ⁻¹⁵	53.2	31.1	39.2 ± 1.7
6	1060	10	8.635	11.3	2.36 × 10 ⁻²	8.25 × 10 ⁻¹⁵	56.7	28.5	38.4 ± 1.6
7	1120	18	8.306	13.2	2.24 × 10 ⁻²	1.97 × 10 ⁻¹⁴	65.3	31.8	41.2 ± 0.9
8	1180	10	7.884	19.1	2.19 × 10 ⁻²	2.19 × 10 ⁻¹⁴	74.8	35.3	43.5 ± 0.8
9	1250	12	7.525	12.4	1.93 × 10 ⁻²	4.10 × 10 ⁻¹⁴	92.5	36.0	42.2 ± 0.6
10	1350	13	24.12	13.7	7.57 × 10 ⁻²	1.735 × 10 ⁻¹⁴	100	11.4	42.8 ± 1.8
95-6-12(a) K-feldspar (J = 0.00866) Total gas age = 14.18 ± 0.37 Ma									
1	450	12	28.63	2.26 × 10 ⁻²	8.95 × 10 ⁻²	2.19 × 10 ⁻¹⁴	0.952	7.5	33.3 ± 2.4
2	500	10	4.389	1.59 × 10 ⁻²	1.24 × 10 ⁻²	6.25 × 10 ⁻¹⁴	3.66	15.9	10.9 ± 0.2
3	500	18	1.385	1.41 × 10 ⁻²	2.76 × 10 ⁻³	4.21 × 10 ⁻¹⁴	5.49	39.5	8.5 ± 0.2
4	550	12	1.589	2.20 × 10 ⁻²	2.95 × 10 ⁻³	1.17 × 10 ⁻¹³	10.6	43.7	10.8 ± 0.1
5	550	37	1.109	3.68 × 10 ⁻²	1.48 × 10 ⁻³	9.52 × 10 ⁻¹⁴	14.7	58.6	10.1 ± 0.1
6	600	13	1.886	6.09 × 10 ⁻²	3.57 × 10 ⁻³	9.69 × 10 ⁻¹⁴	18.9	43.0	12.6 ± 0.1
7	600	15	1.138	7.20 × 10 ⁻²	1.49 × 10 ⁻³	4.84 × 10 ⁻¹⁴	21.0	59.5	10.6 ± 0.2
8	650	12	1.829	5.47 × 10 ⁻²	3.33 × 10 ⁻³	8.48 × 10 ⁻¹⁴	24.7	45.0	12.8 ± 0.1
9	650	30	1.275	3.75 × 10 ⁻²	1.91 × 10 ⁻³	6.51 × 10 ⁻¹⁴	27.5	54.0	10.7 ± 0.2
10	700	18	1.378	1.70 × 10 ⁻²	2.11 × 10 ⁻³	6.16 × 10 ⁻¹⁴	30.2	52.9	11.4 ± 0.2
11	700	31	1.769	1.25 × 10 ⁻²	3.51 × 10 ⁻³	4.08 × 10 ⁻¹⁴	31.9	40.1	11.0 ± 0.3
12	750	13	1.752	1.62 × 10 ⁻²	3.39 × 10 ⁻³	3.30 × 10 ⁻¹⁴	33.4	41.5	11.3 ± 0.3
13	750	23	2.110	1.50 × 10 ⁻²	4.54 × 10 ⁻³	2.80 × 10 ⁻¹⁴	34.6	35.4	11.6 ± 0.4
14	800	10	1.938	3.90 × 10 ⁻²	3.89 × 10 ⁻³	2.37 × 10 ⁻¹⁴	35.6	39.5	11.9 ± 0.5
15	850	14	1.875	6.14 × 10 ⁻²	3.58 × 10 ⁻³	6.34 × 10 ⁻¹⁴	38.4	42.6	12.4 ± 0.2
16	900	10	2.010	3.46 × 10 ⁻²	4.22 × 10 ⁻³	6.88 × 10 ⁻¹⁴	41.4	36.9	11.5 ± 0.2
17	950	9	2.001	3.86 × 10 ⁻²	3.96 × 10 ⁻³	1.07 × 10 ⁻¹³	46.0	40.4	12.6 ± 0.1
18	1000	12	2.068	2.57 × 10 ⁻²	4.01 × 10 ⁻³	2.10 × 10 ⁻¹³	55.1	41.6	13.4 ± 0.1
19	1050	13	2.285	3.83 × 10 ⁻²	4.45 × 10 ⁻³	2.38 × 10 ⁻¹³	65.4	41.5	14.8 ± 0.1
20	1100	17	3.000	3.87 × 10 ⁻²	6.37 × 10 ⁻³	2.85 × 10 ⁻¹³	77.8	36.6	17.1 ± 0.2
21	1125	16	3.388	3.04 × 10 ⁻²	7.63 × 10 ⁻³	2.20 × 10 ⁻¹³	87.4	32.8	17.3 ± 0.2
22	1150	11	3.644	2.32 × 10 ⁻²	8.52 × 10 ⁻³	1.32 × 10 ⁻¹³	93.1	30.3	17.2 ± 0.3
23	1175	16	6.753	3.38 × 10 ⁻²	1.90 × 10 ⁻²	8.27 × 10 ⁻¹⁴	96.7	16.4	17.2 ± 0.4
24	1200	11	13.15	4.09 × 10 ⁻²	4.11 × 10 ⁻²	2.66 × 10 ⁻¹⁴	97.9	7.4	15.0 ± 0.7
25	1225	20	8.809	3.78 × 10 ⁻²	2.52 × 10 ⁻²	1.39 × 10 ⁻¹⁴	98.5	15.3	20.9 ± 0.9
26	1250	13	15.24	3.66 × 10 ⁻²	4.83 × 10 ⁻²	1.09 × 10 ⁻¹⁴	98.9	6.2	14.7 ± 1.3
27	1350	19	21.50	3.74 × 10 ⁻²	6.72 × 10 ⁻²	2.43 × 10 ⁻¹⁴	100	7.5	25.0 ± 1.7
95-6-11(3) K-feldspar (J = 0.00866) Total gas age = 31.33 ± 0.26 Ma									
1	450	24	101.8	3.98 × 10 ⁻²	2.89 × 10 ⁻¹	5.98 × 10 ⁻¹⁵	0.21	16.1	239.5 ± 6.4
2	500	25	4.831	2.53 × 10 ⁻²	1.01 × 10 ⁻²	1.37 × 10 ⁻¹⁴	0.70	37.6	28.2 ± 0.8
3	500	20	3.234	2.70 × 10 ⁻²	5.91 × 10 ⁻³	4.95 × 10 ⁻¹⁵	0.88	45.3	22.7 ± 2.4
4	550	12	2.419	3.80 × 10 ⁻²	2.62 × 10 ⁻³	1.66 × 10 ⁻¹⁴	1.47	67.1	25.2 ± 0.7
5	550	17	2.213	4.12 × 10 ⁻²	2.25 × 10 ⁻³	1.36 × 10 ⁻¹⁴	1.96	68.9	23.7 ± 0.7
6	600	16	2.109	3.84 × 10 ⁻²	1.30 × 10 ⁻³	5.08 × 10 ⁻¹⁴	3.78	80.8	26.4 ± 0.2
7	600	56	2.057	2.60 × 10 ⁻²	1.40 × 10 ⁻³	7.58 × 10 ⁻¹⁴	6.49	78.8	25.2 ± 0.1
8	650	12	1.886	3.55 × 10 ⁻²	4.79 × 10 ⁻⁴	4.99 × 10 ⁻¹⁴	8.27	91.3	26.7 ± 0.2
9	700	11	1.961	3.45 × 10 ⁻²	4.04 × 10 ⁻⁴	1.15 × 10 ⁻¹³	12.38	92.8	28.2 ± 0.1
10	750	12	1.932	2.61 × 10 ⁻²	2.78 × 10 ⁻⁴	1.60 × 10 ⁻¹³	18.09	94.6	28.3 ± 0.1
11	800	13	1.935	2.31 × 10 ⁻²	2.54 × 10 ⁻⁴	1.41 × 10 ⁻¹³	23.12	94.9	28.5 ± 0.1
12	850	18	1.964	1.76 × 10 ⁻²	3.50 × 10 ⁻⁴	1.42 × 10 ⁻¹³	28.20	93.5	28.5 ± 0.1
13	900	10	2.055	1.58 × 10 ⁻²	6.47 × 10 ⁻⁴	9.25 × 10 ⁻¹⁴	31.51	89.5	28.5 ± 0.1
14	950	20	2.106	1.59 × 10 ⁻²	8.45 × 10 ⁻⁴	1.40 × 10 ⁻¹³	36.51	87.0	28.4 ± 0.1
15	1000	12	2.317	2.28 × 10 ⁻²	1.47 × 10 ⁻³	8.93 × 10 ⁻¹⁴	39.70	80.3	28.8 ± 0.1
16	1050	16	2.736	2.00 × 10 ⁻²	2.76 × 10 ⁻³	1.42 × 10 ⁻¹³	44.77	69.3	29.4 ± 0.1
17	1100	11	2.940	2.42 × 10 ⁻²	3.16 × 10 ⁻³	1.93 × 10 ⁻¹³	51.69	67.4	30.7 ± 0.2
18	1130	11	3.289	2.94 × 10 ⁻²	4.20 × 10 ⁻³	2.16 × 10 ⁻¹³	59.41	61.6	31.4 ± 0.1
19	1160	19	2.959	2.38 × 10 ⁻²	2.93 × 10 ⁻³	3.09 × 10 ⁻¹³	70.47	70.0	32.1 ± 0.1
20	1190	15	2.629	1.54 × 10 ⁻²	1.85 × 10 ⁻³	2.79 × 10 ⁻¹³	80.44	78.3	31.9 ± 0.1
21	1220	12	2.502	1.26 × 10 ⁻²	1.44 × 10 ⁻³	2.82 × 10 ⁻¹³	90.51	82.0	31.8 ± 0.1
22	1350	10	2.724	3.09 × 10 ⁻²	2.14 × 10 ⁻³	2.65 × 10 ⁻¹³	100.00	76.0	32.1 ± 0.1

*Radiogenic.

West of the Zedong window at Quxu and Samye, we also see evidence of rapid cooling beginning at ca. 27 Ma (Copeland et al., 1995) that likewise appears related to displacement along the Gangdese thrust. Although the affected rocks occur immediately north of, and structurally beneath the Renbu-Zedong thrust, the observed pattern of cooling (i.e., rapid refrigeration and/or denudation of footwall rocks proximal to the Renbu-Zedong thrust) is opposite to the reheating effects expected if overthrusting of the Renbu-Zedong thrust had been significant. The timing of displacement

along the Gangdese thrust determined from these constraints (Copeland et al., 1995) is broadly consistent with Oligocene deposition of the Luobusha Group in its footwall (Yu and Zheng, 1979).

The timing of displacement of the Renbu-Zedong thrust is constrained in the Lang Xian area east of the mapped area in this study (Fig. 2). Quidelleur et al. (1997) analyzed samples collected from a northeast-southwest traverse in the footwall of the Renbu-Zedong thrust by using ⁴⁰Ar/³⁹Ar and U-Pb techniques. They identified a significant thermal dis-

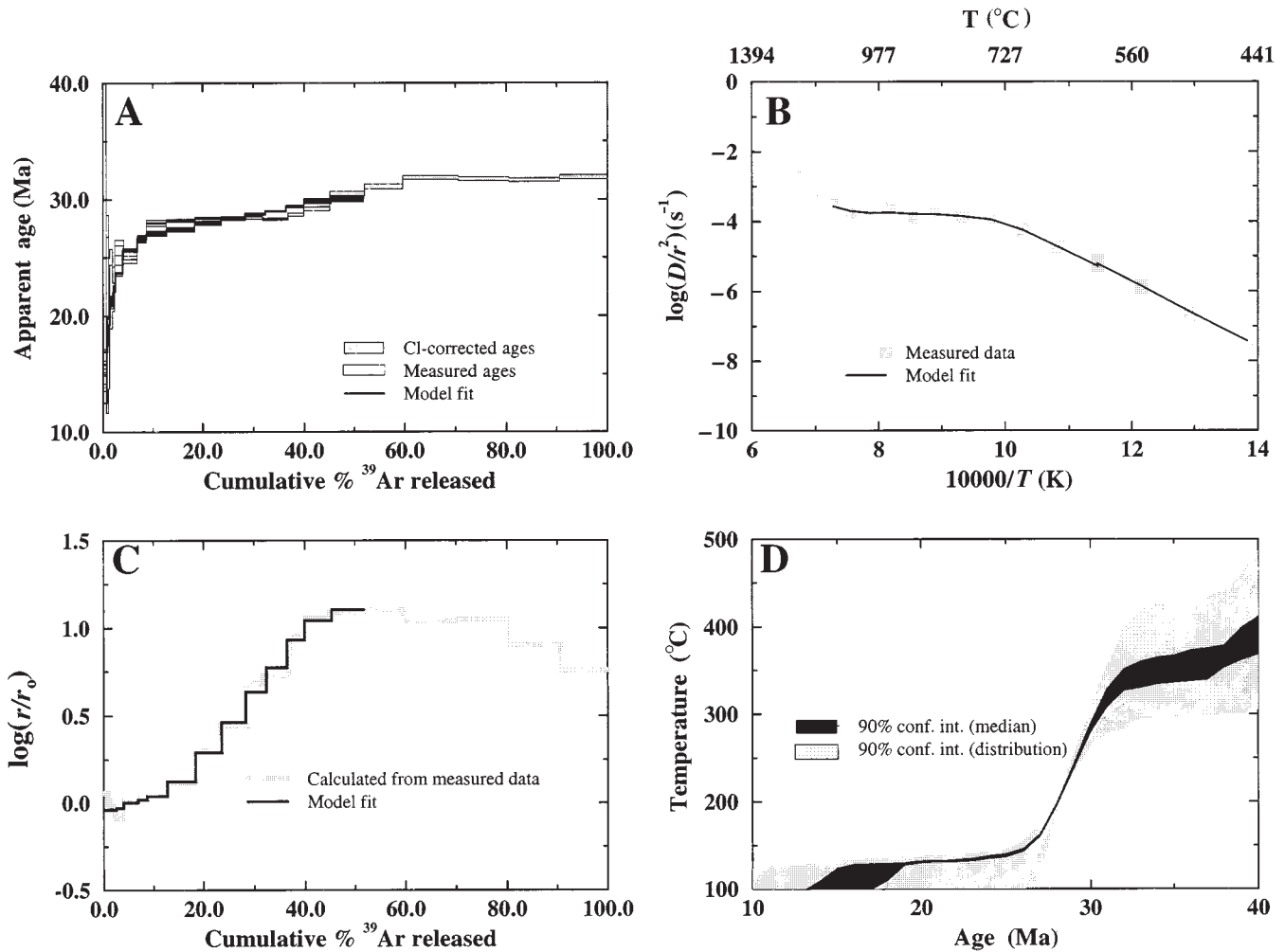


Figure 9. $^{40}\text{Ar}/^{39}\text{Ar}$ step-heating results for K-feldspar from Kailas intrusive complex, sample 95-6-11(3): (A) age spectrum, (B) Arrhenius data, (C) $\log(r/r_0)$ plot, and (D) thermal history. Conf. int.—confidence interval.

turbance, which was attributed to emplacement of the Renbu-Zedong thrust sheet. In particular, $^{40}\text{Ar}/^{39}\text{Ar}$ ages of biotite and K-feldspar increase systematically away from the trace of the Renbu-Zedong thrust, from ca. 12 Ma in the south near the fault to ca. 60 Ma in the north away from the fault. Detailed analysis of K-feldspar $^{40}\text{Ar}/^{39}\text{Ar}$ age spectra and a thermal-model simulation on the effect of the emplacement history of the Renbu-Zedong thrust sheet suggest that the thrust was active between 19 and 10 Ma.

Southwest Tibet (Kailas Area). Constraints on the age of the Kailas thrust can be inferred from the age of the Kailas conglomerate and the age of the Gangdese batholith in the area, which both predate the north-directed thrusts in the Kailas region (Fig. 7). The Kailas igneous complex has been dated by the Rb-Sr whole-rock method at 38.8 ± 1.3 Ma (Honegger et al., 1982). To further understand the timing of the Kailas thrust, we have undertaken $^{40}\text{Ar}/^{39}\text{Ar}$ dating on samples from the Kailas region using standard methods (McDougall and Harrison, 1988). Detailed results are available on the World Wide Web at oro.ess.ucla.edu. A sample of granite from the footwall (95-6-11-3; Figs. 7B and 8) yields a hornblende age of 45.4 ± 1.2 Ma (Table 2; Fig. 8). $^{40}\text{Ar}/^{39}\text{Ar}$ step-heating results for the coexisting K-feldspar (Fig. 9) are interpreted in terms of the multi-diffusion domain model (Lovera et al., 1989) to determine the thermal-history content of the age spectrum. By using recently outlined methods (Harrison et al., 1994; Lovera

et al., 1997; Quidelleur et al., 1997), a good fit to the age spectrum (Fig. 9A), Arrhenius plot (Fig. 9B), and $\log(r/r_0)$ plot (Fig. 9C) were obtained. The resulting thermal history and 90% confidence limits are shown in Figure 9D. Together with the coexisting $^{40}\text{Ar}/^{39}\text{Ar}$ hornblende age, the results indicate emplacement of the granodiorite at an ambient temperature of ~ 400 °C at ca. 45 Ma. At 30 Ma, a phase of rapid cooling began that lasted about 5 m.y. (Table 2; Fig. 9D). We infer this rapid cooling episode to be due to slip on a structure equivalent to the Gangdese thrust that had the effect of refrigerating the hanging-wall granitoid.

Until recently, age assessment of the Kailas conglomerate (late Eocene to Miocene?) has been problematic (Gansser, 1964). By using thermochronometry to establish an upper limit for derivation from the Gangdese basement and dating crosscutting dikes to constrain a lower bound, the age of deposition of the Kailas conglomerate and its equivalent along the Yalu River valley has been estimated at three locations in western, central, and eastern Tibet (Harrison et al., 1993; Ryerson et al., 1995). At all three sites, the results are consistent with a late Oligocene–early Miocene (30–17 Ma) age of deposition.

As described above, the upper part of the Kailas conglomerate consists of cobbles of metamorphic schists, volcanic breccias, and purple and green sandstones that are characteristic of the hanging wall of the South Kailas thrust system. This stratigraphic relationship suggests that at least during the

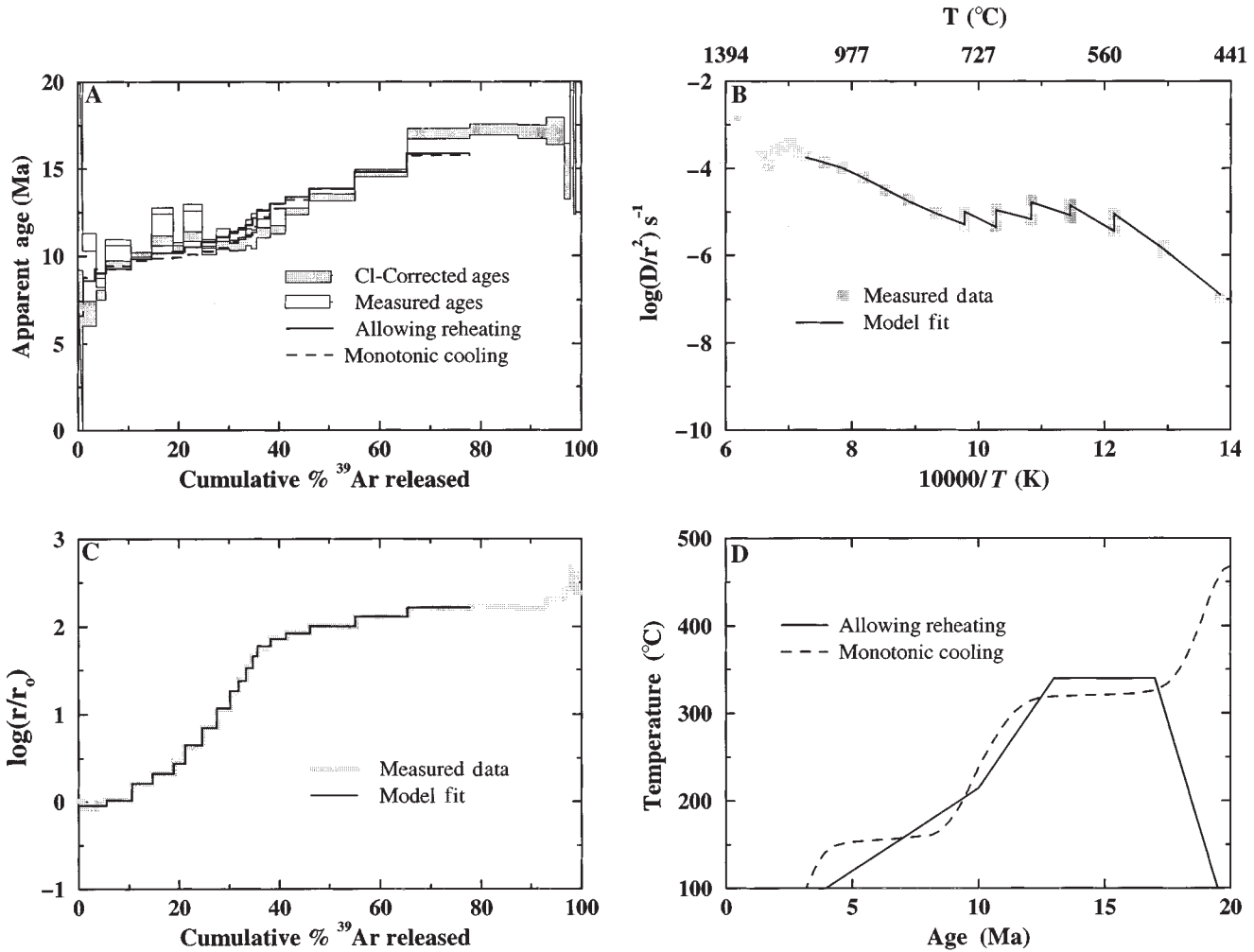


Figure 10. $^{40}\text{Ar}/^{39}\text{Ar}$ step-heating results for K-feldspar from a cobble of the Kailas conglomerate, sample 95-6-12(1a): (A) age spectrum showing fit for reheating condition, (B) Arrhenius data, (C) $\log(r/r_0)$ plot, and (D) thermal histories for monotonic cooling and reheating models.

deposition of the uppermost part of the Kailas conglomerate, the South Kailas thrust system was active. Thus, the depositional age of the Kailas conglomerate broadly implies that the age of the South Kailas thrust system is middle Miocene.

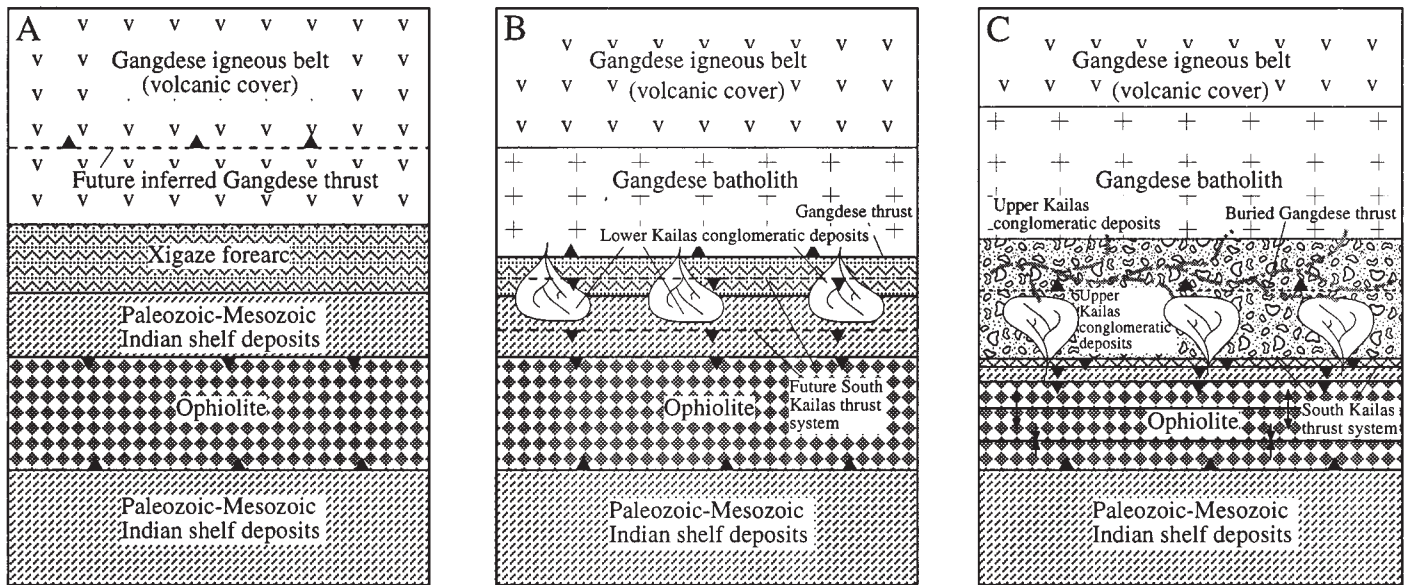
A constraint on the timing of backthrusting is provided by $^{40}\text{Ar}/^{39}\text{Ar}$ thermochronologic results for a K-feldspar separate from a volcanic cobble in the Kailas conglomerate, directly below the frontal thrust of the South Kailas thrust system. In this case, a good fit to the age spectrum (Fig. 10A, Table 2) was determined by assuming that the sample had undergone a thermal event. A good model fit was obtained by assuming that a temperature of ~ 350 °C was reached at 19 Ma and remained at that value until ca. 13 Ma when cooling at a rate of ~ 60 °C/m.y. began (Fig. 10D). Although an equally good fit could be obtained by assuming a slow cooling history (also shown in Fig. 10D), the origin of this sample as a cobble within the footwall of a thrust leads us to prefer the reheating interpretation in which the thermal pulse reflects footwall heating during slip along the South Kailas thrust (see Fig. 7B). Because the South Kailas thrust system is offset by the right-slip Karakoram fault in Gar Valley (Cheng and Xu, 1987; Fig. 6), the thrust must predate the Karakoram fault. Searle (1996b) inferred that movement on the Karakoram fault was initiated at ca. 4 Ma, an estimate based on its total offset (<120 km) divided by its current slip rate (~ 30 mm/yr). If this age esti-

mate is correct, the activity of the South Kailas thrust is bracketed to be younger than 20 Ma but older than 4 Ma. This age constraint on the Kailas thrust implies that it is coeval with the activity along the Renbu-Zedong thrust in southeast Tibet (Fig. 7B, sample 95-6-12(a)) (Quidelleur et al., 1997) and development of the South Tibetan detachment system (Burchfiel et al., 1992; Edwards and Harrison, 1997).

DISCUSSION

Cenozoic Structural Evolution of the Kailas Area

The suture zone in the Zedong and Kailas areas share key similarities in structural relationships and timing of deformation. Both areas have a major south-dipping thrust juxtaposing Tethyan strata on top of the Gangdese batholith. The faults were active between 20 and 4 Ma in the Kailas area and between 19 and 10 Ma in the Zedong–Lang Xian area. The footwalls of both south-dipping thrusts have a conglomerate unit containing clasts that are dominantly derived from the granitoids and wall rocks of the Gangdese batholith. Moreover, the Gangdese basement adjacent to the two areas is characterized by early Miocene rapid cooling (Harrison et al., 1992, 1993; Copeland et al., 1995). The apparent lack of surface exposure of the



Stage 1 (50–30 Ma): Initiation of the Gangdese thrust system in southwest Tibet

Stage 2 (30–20 Ma): Development of the Gangdese thrust system in southwest Tibet that causes denudation of the southern Gangdese batholith

Stage 3 (20–4 Ma): Development of the South Kailas thrust system that induces deposition of upper Kailas conglomerate

Figure 11. Cenozoic geologic evolution of the Kailas region, depicted via schematic maps. (A) Stage 1 (50–30 Ma). A large ophiolitic complex, described by Heim and Gansser (1939), had already been emplaced over the Paleozoic–Mesozoic Indian shelf sequence. The exact time of emplacement is not known. The future inferred Gangdese thrust began forming in the southern part of the Gangdese igneous belt. **(B) Stage 2 (30–20 Ma).** Movement on the inferred Gangdese thrust exposed rocks of the Gangdese batholith in the thrust hanging wall. As its southward displacement increased, the thrust eventually placed the Gangdese batholith over the Xigaze forearc strata. Synchronous with thrusting was the deposition of both volcanic and granitic cobbles eroded from the hanging wall on top of the Xigaze forearc strata in the footwall. As a result of southward movement of the Gangdese thrust sheet, the exposed width of the Xigaze forearc basin was reduced. The future south-dipping South Kailas thrust system was initiated within both the Xigaze forearc strata (the northern thrust in the map) and the Paleozoic–Mesozoic Indian continental shelf strata (the southern thrust in the map). **(C) Stage 3 (20–4 Ma).** Movement along the Gangdese thrust ceased at ca. 20 Ma. The south-dipping South Kailas thrust system became fully developed, which caused denudation of both the Xigaze forearc sedimentary sequence and the Indian shelf deposits in the thrust system's hanging wall. Sediments derived from both the hanging wall and the footwall of the thrust system contributed to the deposition of the upper Kailas conglomerate that buried the older Gangdese thrust. A minor component of the sediments in the upper Kailas conglomerate was derived from the Gangdese batholith from the north. Movement along the South Kailas thrust system caused deformation in its hanging wall, which deformed the older thrust that was carrying the ophiolite.

Gangdese thrust in the Kailas area leads us to consider possible alternative explanations. If the thrust never developed in this area, then the absence of the Xigaze forearc basin may be related to other causes such as displacement along a large strike-slip fault (Peltzer and Tapponnier, 1988). Although basement uplift adjacent to large-displacement strike-slip faults may occur (Leloup et al., 1995), the lack of evidence for compatible deformation in the Gangdese batholith does not argue strongly for this mechanism. A role for normal faulting can be excluded on similar grounds. Therefore, although field evidence for thrusting is lacking, the most likely explanation for localized denudation of the Gangdese granite in the Kailas area is south-directed thrusting that occurred along a fault now buried beneath the hanging wall of the South Kailas thrust system. Such an interpretation is supported by the existence of a south-directed thrust in the Kailas area (fault (d) in Fig. 7B), which could be part of the early south-directed thrust system. In addition, this interpretation is also consistent with the presence of south-directed Tertiary thrusts in the Shiquanhe area (~150 km northwest of Mount Kailas, Figs. 2 and 6), which cut Cretaceous and early Tertiary plutonic and volcanic rocks (Fig. 6; Cheng and Xu, 1987; Liu et al., 1988; Matte et al., 1996). As the 14–12 Ma felsic volcanic rocks in the area immediately west and north of

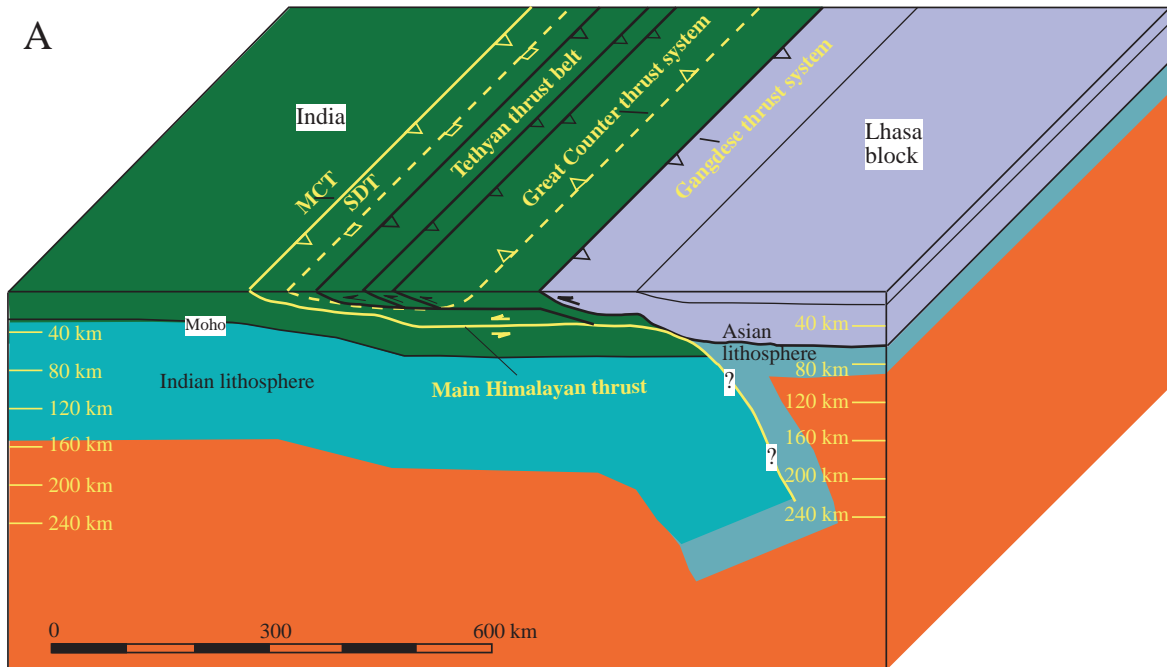
Kailas are flat lying (Miller et al., 1996), the north-dipping Tertiary thrusts in the Shiquanhe area are likely late Oligocene to early Miocene in age, a period overlapping the age duration of the Gangdese thrust in southeast Tibet but predating the activity of the South Kailas thrust system.

On the basis of the aforementioned geologic relationships and geochronological constraints, we propose a kinematic model for the tectonic development of the South Kailas thrust system (Fig. 11). The reconstruction of the Gurla Mandhata detachment system and the Karakoram fault system in southwestern Tibet are based on studies of Yin et al. (1996), Murphy et al. (1997), and Searle et al. (1996b).

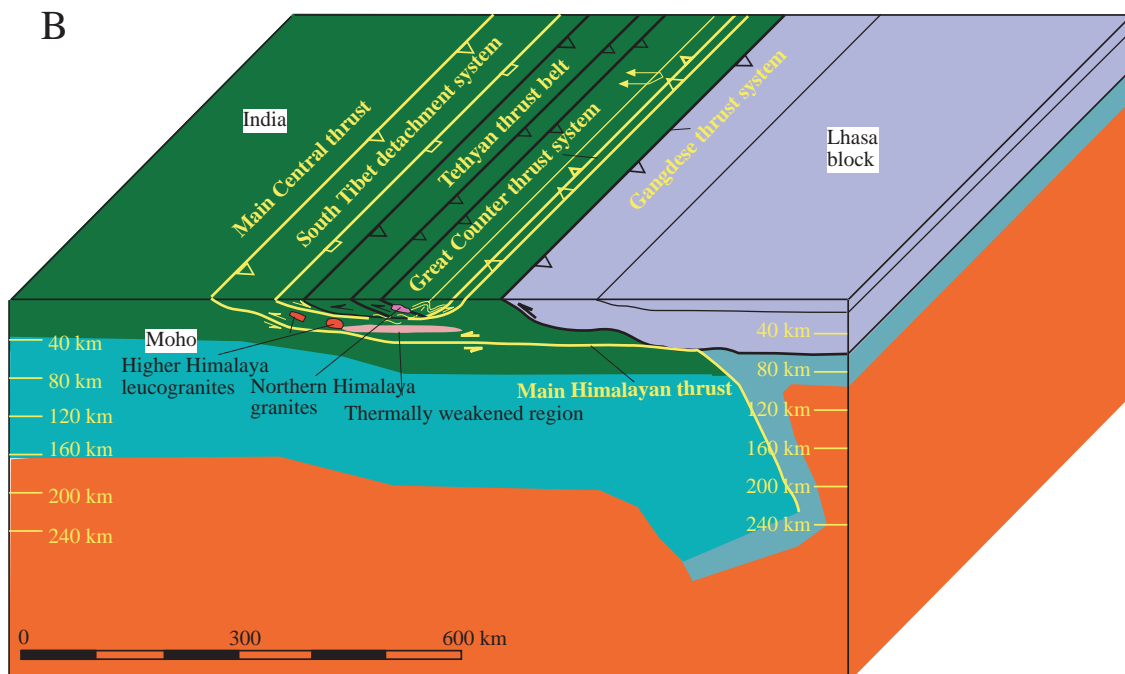
Stage 1 (50–30 Ma) (Fig. 11A). A large ophiolitic complex, described by Heim and Gansser (1939), was already emplaced over the Paleozoic–Mesozoic Indian shelf sequence. Its exact age of emplacement is not known. The future inferred Gangdese thrust was initiated in the southern part of the Gangdese igneous belt.

Stage 2 (30–20 Ma) (Fig. 11B). Movement on the inferred Gangdese thrust exposed rocks of the Gangdese batholith in the thrust hanging wall. As its southward displacement increased, the thrust eventually placed the Gangdese batholith over the Xigaze forearc strata. Synchronous with thrust-

Stage 1 (30–20 Ma): Crust thickening in northern Himalaya and south Tibet due to motion along the Gangdese thrust system, Main Central thrust, and the Tethyan thrust belt. The Great Counter thrust system will be initiated above the thickened crust between the Gangdese thrust system and the Main Central thrust.



Stage 2 (20–10 Ma): Development of the Great Counter thrust system and emplacement of the Himalayan leucogranites between the Main Central thrust and the Gangdese thrust as a result of thermal heating and weakening of the middle and lower crust in northern Himalaya and south Tibet. Synchronous development of the South Tibet detachment system resulted from gravitational spreading of the thick crustal root. Continuing development of the Main Central thrust.



ing was the deposition of both volcanic and granitic cobbles eroded from the hanging wall on top of the Xigaze forearc strata in the footwall. As a result of southward movement of the Gangdese thrust sheet, the exposed width of the Xigaze forearc basin is reduced. The future south-dipping South Kailas thrust system was initiated within both the Xigaze forearc strata (the northern thrust in Fig. 11b) and the Paleozoic-Mesozoic Indian continental shelf strata (the southern thrust in Fig. 11b).

Stage 3 (20–4 Ma) (Fig. 11C). Movement along the Gangdese thrust ceased at ca. 20 Ma. The south-dipping South Kailas thrust system became fully developed, which caused denudation of both the Xigaze forearc sedimentary sequence and the Indian shelf deposits in its hanging wall. Sediments derived from both the hanging wall and the footwall of the thrust system contributed to the deposition of the upper Kailas conglomerate that buried the older Gangdese thrust. A minor component of the sediments in the upper Kailas conglomerate was derived from the Gangdese batholith from the north. Movement along the South Kailas thrust system caused deformation in its hanging wall, which deformed the older thrust carrying the ophiolite.

Origin of the Gangdese and Great Counter Thrusts

The greatest puzzle arising from this and previous investigations is why the Gangdese thrust, the earliest postcollisional crustal-thickening feature documented in southern Tibet, developed at ca. 30 Ma, ~20–25 m.y. after the initial collision between India and Asia (Le Fort, 1996). Similarly, why were Tethyan strata thrust over the Gangdese batholith along the south-dipping Great Counter thrust system subsequent to termination of the Gangdese thrust? The last question is particularly important because the Great Counter thrust system developed during the period in which the Main Central thrust had already accommodated at least 100 km of slip (e.g., Schelling, 1992; Srivastava and Mitra, 1994; Lyon-Caen and Molnar, 1985; Hauck et al., 1998). Why, then, did coeval thrusting take place within the hinterland in contrast to the general pattern of progression of the Himalayan thrusting toward the foreland during the early and middle Miocene?

Gangdese Thrust. An analysis of regional tectonic events suggests that several major Tertiary fault systems in central Asia were initiated during the Oligocene and thus may be kinematically linked. Sedimentologic, biostratigraphic, and magnetostratigraphic data from the western Kunlun Shan and the Nan Shan (Fig. 1) suggest that Tertiary shortening began there between 30 and 26 Ma (Ye and Huang, 1990; Rumelhart et al., 1997; Wang and Burchfiel, 1997). The southern margin of the Qaidam basin (Fig. 1) records a major transition in depositional setting during the Oligocene suggestive of an emerging topographic highstand, perhaps related to crustal shortening (Hansen, 1997). The significant variation in thickness of the Oligocene strata across the major Tertiary thrusts in southern Qaidam also suggests that the time of initial crustal shortening occurred during the late Oligocene

(Hansen, 1997; Song and Wang, 1993; Gu, 1987). Although somewhat younger, sedimentary records in conjunction with biostratigraphy (Ye and Huang, 1990; Allen et al., 1991; Avouac et al., 1993; Yin et al., 1998), magnetostratigraphy (Craig, 1995; Yin et al., 1998), and apatite fission-track ages (Hendrix et al., 1994) suggest that thrusting in the Chinese Tian Shan began between 24 and 21 Ma (Yin et al., 1998; Craig, 1995).

The regional pattern of increased intensity of north-south shortening in both the southern (Gangdese thrust) and northern parts (Kunlun and Nan Shan) of the Tibetan Plateau and the Tian Shan suggests a change in stress distribution throughout south-central Asia at this time. One possible explanation for this widespread phenomenon is an increase in the compressive deviatoric stress component in the north-south direction, which may have been caused by (1) an increase in convergence rate between India and Asia, (2) a decrease in convergence rate between the Eurasian and Pacific plates, or (3) a change in convergence direction or magnitude of tractions across the two plate boundaries (e.g., Kong et al., 1997).

The convergence history between Asia and India has been examined by several workers (Patriat and Achache, 1984; Besse and Courtillot, 1988; Dewey et al., 1989; Le Pichon et al., 1992; Northrup et al., 1995). Since 45 Ma, the convergence rate was relatively uniform at about 5 cm/yr (Dewey et al., 1989). Similarly, the convergence rate between the Eurasian and Pacific plates was relatively constant, although an ~20° counterclockwise rotation in convergence direction between the two plates occurred in the Oligocene (Engelbreton et al., 1985). As shown by Kong et al. (1997), the strain distribution in Asia could be very sensitive to small changes in traction on the Indo-Asian and Pacific-Asian convergent boundaries. It is possible that the change in convergence direction between Asia and the Pacific at this time triggered a change in the plate-boundary tractions between Asia and India and between Asia and the Pacific that in turn produced a strong north-south compressive stress and shortening in central Asia.

In addition to the change in the regional stress condition that resulted in initiation of the Gangdese thrust system, the local thermal regime may have also influenced its development. As documented by Harrison et al. (in press), magmatic input to the Gangdese batholith in southeastern Tibet continued until 30 Ma. This magmatism implies that the crust in the Gangdese Shan may have remained relatively hotter compared to the regions to the north immediately prior to the initiation of movement on the Gangdese thrust. However, this interpretation does not explain why movement on the Gangdese thrust did not begin earlier, as the region occupied by the Gangdese batholith was likely anomalously hot, and thus weak, immediately after the closure of the Indus-Tsangpo suture zone.

Great Counter Thrust System along the Indus–Yalu River Valleys. Activity along the Great Counter thrust system in the Tethyan Himalaya suggests that it was coeval or overlapped in time with (1) slip on the South Tibetan detachment system (Burchfiel et al., 1992; Edwards and Harrison,



Figure 12. Tectonic evolution of the Great Counter thrust system. (A) Stage 1 (30–20 Ma). It is possible that thrusting along the Main Central thrust during its early phase of movement in the early Miocene–middle Miocene (Harrison et al., 1992; Hauck et al., 1998; cf. Hodges et al., 1994) and north-south crustal shortening in the Tethyan Himalaya in late Eocene and early Oligocene time (Ratschbacher et al., 1994) produced a thick crustal root in the northern Himalayan region and southern Tibet. In addition, it is possible that movement along the Gangdese thrust also produced a thick crustal root beneath the southernmost Lhasa block. **(B) Stage 2 (20–10 Ma).** Thermal relaxation of this thickened crust (England and Thompson, 1984), shear heating along major thrusts (Molnar and England, 1990; Harrison et al., 1997a), muscovite-breakdown melting during decompression (e.g., Searle et al., 1997a), or a combination of these processes may have caused thermal weakening and locally partial melting of the crust in the Himalayan and southern Tibetan regions. As a consequence, a ductility contrast (i.e., strength contrast) was created between the thickened and heated region in south Tibet in the middle and the cooler Lhasa block and India to the north and south, respectively. Under the north-south compression, the plastic and more buoyant lower-crustal root in the Himalaya and southernmost Tibet may have been displaced both upward and laterally. The inferred upward movement of the ductile lower-crustal root beneath southernmost Tibet may have been manifested by the emplacement of North Himalayan gneiss domes and granites. The upward movement of the lower crust due to horizontal shortening may have been accompanied by thrusting along the Main Central thrust and the development of the Great Counter thrust system.

1997), (2) emplacement of the North Himalayan granites and gneiss domes (Schärer and Allègre, 1986; Harrison et al., 1997a), and (3) slip on the Main Boundary thrust (Burbank et al., 1996). In contrast to the Gangdese thrust, which affects granitic basement, the Great Counter thrust system is a thin-skinned thrust system, i.e., significant shortening in the thrust system was accommodated by shortening of sedimentary cover rocks via folding or imbricate thrusting in its hanging wall. The imbricate style of such deformation is emphasized in the mapping of the central Tethyan Himalaya by Ratschbacher et al. (1994). Intense folding in the hanging wall of the Great Counter thrust system is also documented in this study in the Zedong area.

Tectonic Model

The occurrence of the contemporaneous crustal shortening in the Himalaya and southern Tibet described above leads us to propose a kinematic model for the development of the Main Central thrust, the Himalayan leucogranites, South Tibet detachment fault, and the Great Counter thrust system (Fig. 12). The model is based on geologic observations discussed in this study and those presented by earlier workers (e.g., Schelling, 1992; Ratschbacher et al., 1992; Harrison et al., 1992; Yin et al., 1994). The inferred deep-crustal structure in the model is based on recent results of the Project INDEPTH (Makovsky et al., 1996; Hauck et al., 1998; Alsdorf et al., 1998) and the synthesis of seismological observations and interpretations of the Tibetan Plateau of Owens and Zandt (1997).

Stage 1 (30–20 Ma) (Fig. 12A). Early Miocene to middle Miocene movement of the Main Central thrust (Harrison et al., 1992, 1997b; Hauck et al., 1998) and late Eocene–early Oligocene north-south crustal shortening in the Tethyan Himalaya (Ratschbacher et al., 1994) would produce a thick crustal root in the northern Himalaya and southern Tibet. In addition, movement along the Gangdese thrust may also have produced a thick crustal root beneath the southernmost Lhasa block.

Stage 2 (20–10 Ma) (Fig. 12B). Thermal relaxation of this thickened crust (England and Thompson, 1984), shear heating along major thrusts (Molnar and England, 1990; Harrison et al., 1997b), decompression melting during normal faulting (e.g., Harris and Massey, 1994), or a combination of these processes may have caused thermal weakening of the lower crust in the Himalayan and southern Tibetan regions. As a consequence, a strength contrast would have been created between the thickened and heated region of southern Tibet relative to India and the Lhasa block. Under the north-south compression, the plastic and more buoyant lower-crustal root in the Himalaya and southernmost Tibet may have been displaced both upward and laterally.

The inferred upward movement of the ductile lower-crustal root beneath southernmost Tibet may have been manifested by the emplacement of North Himalayan gneiss domes and granites. The upward movement of the lower crust due to horizontal shortening may have been accompanied by thrusting along the Main Central thrust and the development of the Great Counter thrust system.

This proposed mechanism is similar to that for the development of the Mesozoic North American Cordilleran fold-and-thrust belt, where ductility contrast between the magmatic arc to the west and the cratonic crust and its cover strata to the east is considered to be the key controlling factor for its formation (e.g., Burchfiel and Davis, 1975).

Structural Modification of the Indus-Tsangpo Suture Zone during the Indo-Asian Collision

Suture zones have been regarded as a diagnostic feature recording the prior existence of an ocean between two collided continents (e.g., Dewey and Burke, 1973). However, recognizing the existence of a suture zone may be difficult because suture zones can be significantly modified during sub-

sequent deformation (see discussion by Şengör and Natal'in, 1996). Our study along one of the better-known suture zones provides some insight into how these features can be modified during the course of continuing continental collision. Note that if the hanging wall of the Great Counter thrust system had moved ~30–50 km farther to the north, a relatively modest amount compared to the magnitude of thrusting in the Himalaya, no physical evidence of the suture would have been observable at the surface.

CONCLUSIONS

Geologic mapping and geochronological analysis in southwest Tibet (Kailas area) and southeast Tibet (Zedong area) clearly document two episodes of crustal shortening along the classic Indus-Tsangpo “suture” in the Yalu River valley. The older event occurred between ca. 30 Ma and 24 Ma during movement along the north-dipping Gangdese thrust. The development of the Gangdese thrust caused extensive, localized denudation of the Gangdese batholith in its hanging wall and subduction of the Xigaze forearc strata in its footwall in southeast and southwest Tibet. Examination of the timing of major tectonic events in southern Asia suggests that the initiation of the Gangdese thrust was coeval with the initiation and development of major fault systems, such as the Nan Shan, the western Kunlun Shan, and the Tian Shan thrust belts during the late Oligocene. Within this time interval, the convergence direction between the Eurasian and Pacific plates abruptly changed by about 20°. This change may have altered the force balance along the plate boundaries, which in turn could have intensified the north-south compressive stress in central Asia. The younger north-south shortening event along the south-dipping Great Counter thrust system occurred between 19 Ma and 10 Ma along the Indus and Yalu River valleys in southern Tibet. The coeval development of this thrust and the North Himalayan granite belt may reflect weakening of the Himalayan crust due to either thermal relaxation of a thickened crust during the early phase of collision between India and Asia or shear heating along major thrusts.

ACKNOWLEDGMENTS

This work was supported by a National Science Foundation grant (EAR-9316176), Department of Energy grant DE-FG-03-89ER14049, and a grant from the Lawrence Livermore National Laboratory Institute of Geophysics and Planetary Physics (to Ryerson) operating under the auspices of DOE contract W-7405-Eng-48. Insightful and constructive comments by Lothar Ratschbacher, Guatam Mitra, and Peter Copeland improved the original manuscript.

REFERENCES CITED

- Allègre, C. J., and 34 others, 1984, Structure and evolution of the Himalaya-Tibet orogenic belt: *Nature*, v. 307, p. 17–22.
- Allen, M. B., Windley, B. F., Zhang Chi, Zhao Zhongyan, and Wang Guangrei, 1991, Basin evolution within and adjacent to the Tien Shan range, NW China: *Geological Society [London] Journal*, v. 148, p. 369–378.
- Alsdorf, D., Brown, L., Nelson, K. D., Makovsky, Y., Klempner, S., and Zhao, W., 1998, Crustal deformation of the Lhasa terrane, Tibet plateau, from Project INDEPTH deep seismic reflection profiles: *Tectonics*, v. 17, p. 501–519.
- Argand, E., 1924, *Le Tectonique de l'Asie*, in *Proceedings of the Thirteenth International Geological Congress*, p. 171–372, Brussels.
- Arnaud, N. O., Vidal, P., Tapponnier, P., Mate, P., and Deng, W. M., 1992, The high K₂O volcanism of northwestern Tibet, Geochemistry and tectonic implications. *Earth and Planetary Science Letters*, v. 111, p. 351–367.
- Avouac, J. P., and Burov, E. B., 1996, Erosion as a driving mechanism of intracontinental mountain growth: *Journal of Geophysical Research*, v. 101, p. 17747–17969.
- Avouac, J. P., Tapponnier, P., Bai, M., You, H., and Wang, G., 1993, Active thrusting and folding along the northern Tien Shan and late Tertiary rotation of the Tarim relative to Dzungaria and Kazakhstan: *Journal of Geophysical Research*, v. 98, p. 6755–6804.
- Besse, J., and Courtillot, V., 1988, Paleogeographic maps of the continents bordering the Indian Ocean since the Early Jurassic: *Journal of Geophysical Research*, v. 93, p. 1791–1808.
- Bird, P., 1991, Lateral extrusion of lower crust from under high topography in the isostatic limit:

- Journal of Geophysical Research, v. 96, p. 10275–10286.
- Briais, A., Patriat, P., and Tapponnier, P., 1993, Updated interpretation of magnetic anomalies and seafloor spreading stages in the South China Sea: Implications for the Tertiary tectonics of SE Asia: *Journal of Geophysical Research*, v. 98, p. 6299–6328.
- Burbank, D. W., Beck, R. A., and Mulder, T., 1996, The Himalayan foreland basin, *in* Yin, A., and Harrison, T. M., eds., *The tectonics of Asia*: New York, Cambridge University Press, p. 149–188.
- Burchfiel, B. C., and Davis, G. A., 1975, Nature and controls of Cordillera orogenesis, western United States: Extension of an earlier synthesis: *American Journal of Science*, v. 275-A, p. 363–395.
- Burchfiel, B. C., Deng, Q., Molnar, P., Royden, L. H., Wang, Y., Zhang, P., and Zhang, W., 1989, Intracrustal detachment within zones of continental deformation: *Geology*, v. 17, p. 748–752.
- Burchfiel, B. C., Chen Zhiliang, Hodges, K. V., Liu Yuping, Royden, L. H., Deng, C., and Xu, J., 1992, The South Tibetan detachment system, Himalayan orogen: Extension contemporaneous with and parallel to shortening in a collisional mountain belt: *Geological Society of America Special Paper* 269, p. 1–41.
- Burg, J. P., compiler, 1983, *Carte géologique du sud du Tibet*: Paris, Institut National d'Astronomie et de Géophysique, Centre Nationale de la Recherche, Sci. scale 1:500 000.
- Burg, J. P., and Chen, G. M., 1984, Tectonics and structural zonation of southern Tibet, China: *Nature*, v. 311, p. 219–223.
- Burg, J. P., Leyreloup, A., Girardeau, J., and Chen, G. M., 1987, Structure and metamorphism of a tectonically thickened continental crust: The Yalo Tsangpo suture zone (Tibet): *Royal Society of London Philosophical Transactions*, ser. A, v. 321, p. 67–86.
- Chang Chengfa and Zheng Xilang, 1973, Structural characteristics of southern Tibet and the Jumulangma region: *Scientia Geologica Sinica*, v. 1973, p. 1–12.
- Chang and 26 others, 1986, Preliminary conclusions of the Royal Society and Academia Sinica 1985 Geotraverse of Tibet: *Nature*, v. 323, p. 501–507.
- Cheng Jiaxiang and Xu Guozhang, 1987, Geologic map at a scale of 1:1 000 000 and geologic report of the Gedake region, Tibetan Bureau of Geology and Mineral Resources, 363 p.
- Chung, S. L., Lo, C. H., Lee, T. Y., Zhang, Y., Xie, Y., Li, X., Wang, K. L., and Wang, P. L., 1998, Diachronous uplift of the Tibetan Plateau starting 40 Myr ago: *Nature*, v. 394, p. 769–773.
- Copeland, P., Harrison, T. M., Pan Yun, Kidd, W. S. F., Roden, M., and Zhang Yuquan, 1995, Thermal evolution of the Gangdese batholith, southern Tibet: A history of episodic unroofing: *Tectonics*, v. 14, p. 223–236.
- Coulon, C., Maluski, H., Bolling, C., and Wang, S., 1986, Mesozoic and Tertiary rocks from central and southern Tibet: $^{40}\text{Ar}/^{39}\text{Ar}$ dating, petrologic characteristics and geodynamic significance: *Earth and Planetary Science Letters*, v. 79, p. 281–302.
- Craig, P. A., 1995, Tertiary development of the Kuche foreland of the Tarim basin, Xinjiang, China [Master's thesis]: Los Angeles, University of California, 198 p.
- Deng, W. M., 1978, A preliminary study on the petrology and petrochemistry of the Quaternary volcanic rocks of the northern Tibet autonomous region: *Acta Geologica Sinica*, v. 52, p. 148–162 (in Chinese).
- Deniel, C., Vidal, Ph., Fernandez, A., Le Fort, P., and Peucat, J.-J., 1987, Isotopic study of the Manaslu granite (Himalaya, Nepal): Inferences on the age and source of Himalayan leucogranites: *Contributions to Mineralogy and Petrology*, v. 96, p. 78–92.
- Dewey, J. F., and Burke, K., 1973, Tibetan, Variscan and Precambrian basement reactivation: Products of continental collision: *Journal of Geology*, v. 81, p. 683–692.
- Dewey, J. F., Cande, S., and Pitman, W. C., 1989, Tectonic evolution of the India/Eurasia collision zone: *Eclogae Geologicae Helveticae*, v. 82, p. 717–734.
- Durr, S. B., 1996, Provenance of Xigaze fore-arc basin clastic rocks (Cretaceous, south Tibet): *Geological Society of American Bulletin*, v. 108, p. 669–684.
- Edwards, M. A., and Harrison, T. M., 1997, When did the roof collapse? Late Miocene north-south extension in the High Himalaya revealed by Th-Pb monazite dating of the Khula Kangri granite: *Geology*, v. 25, p. 543–546.
- Engelbreton, D. C., Cox, A., and Gordon, R. G., 1985, Relative motions between oceanic and continental plates in the Pacific basin: *Geological Society of America Special Paper* 206, 59 p.
- England, P., and Houseman, G., 1986, Finite strain calculations of continental deformation: 2. Comparison with the India-Asia collision zone: *Journal of Geophysical Research*, v. 91, p. 3664–3676.
- England, P., and Thompson, A. B., 1984, Pressure-temperature-time paths of regional metamorphism: Part I. Heat transfer during the evolution of regions of thickened continental crust: *Journal of Petrology*, v. 25, p. 894–928.
- Gaetani, M., and Garzanti, E., 1991, Multicyclic history of the northern India continental margin (northwestern Himalaya): *American Association of Petroleum Geologists Bulletin*, v. 75, p. 1427–1446.
- Gansser, A., 1964, *The geology of the Himalayas*: New York, Wiley Interscience, 289 p.
- Girardeau, J., Marcous, J., and Zao, Y., 1984, Lithologic and tectonic environment of the Xigaze ophiolite (Yarlung Zangbo suture zone, southern Tibet, China), the kinematics of its emplacement: *Eclogae Geologicae Helveticae*, v. 77, p. 153–170.
- Gu Susong, chief editor, 1987, *Oil fields, in The Qinghai-Xizang region*: Beijing, Petroleum Publishing House, Publication of Chinese Petroleum Geology Series, v. 14, 483 p.
- Hansen, A. D., 1997, Evidence of Cenozoic erosional unroofing adjacent to the northern Qaidam basin, NW China, preserved within basin margin strata: *Geological Society of America Abstracts with Programs*, v. 29, no. 6, p. A143.
- Harris, N., and Massey, J., 1994, Decompression and anatexis of Himalayan metapelites: *Tectonics*, v. 13, p. 1537–1546.
- Harrison, T. M., Copeland, P., Kidd, W. S. F., and Yin, A., 1992, Raising Tibet: *Science*, v. 255, p. 1663–1670.
- Harrison, T. M., Copeland, P., Hall, S. A., Quade, J., Burner, S., Ojha, T. P., and Kidd, W. S. F., 1993, Isotopic preservation of Himalayan/Tibetan uplift, denudation, and climate histories of two molasse deposits: *Journal of Geology*, v. 100, p. 157–175.
- Harrison, T. M., McKeeagan, K. D., and Le Fort, P., 1995, Detection of inherited monazite in the Manaslu leucogranite by $^{208}\text{Pb}/^{232}\text{Th}$ ion microprobe dating: Crystallization age and tectonic implications: *Earth and Planetary Science Letters*, v. 133, p. 271–282.
- Harrison, T. M., Leloup, P. H., Chen Wenji, Ryerson, J. F., and Tapponnier, P., and Lacassin, R., 1996, Diachronous initiation of transtension along the Ailao Shan–Red River shear zone, Yunnan and Vietnam, *in* Yin, A., and Harrison, T. M., eds., *The tectonics of Asia*: New York, Cambridge University Press, p. 208–226.
- Harrison, T. M., Lovera, O. M., and Grove, M., 1997a, New insights into the origin of the two contrasting Himalayan granite belts: *Geology*, v. 25, p. 899–902.
- Harrison, T. M., Ryerson, F. J., Le Fort, P., Yin, A., and Lovera, O. M., 1997b, A late Miocene–Pliocene origin of the central Himalayan inverted metamorphism: *Earth and Planetary Science Letters*, v. 146, p. E1–E8.
- Harrison, T. M., Yin, A., Grove, M., Lovera, O. M., and Ryerson, F. J., Displacement history of the Gangdese thrust, Zedong window, southeastern Tibet: *Journal of Geophysical Research* (in press).
- Hauck, M. L., Nelson, K. D., Brown, L. D., Zhao Wenjin, and Ross, A. R., 1998, Crustal structure of the Himalayan orogen at $\sim 90^\circ$ east longitude from Project INDEPTH deep reflection profiles: *Tectonics*, v. 17, p. 481–500.
- Heim, A., and Gansser, A., 1939, Central Himalaya, geological observations of the Swiss expedition 1936: *Memoires de la Societe Helvetique des Sciences Naturelles*, v. 63, 245 p.
- Hendrix, M. S., Dumitru, T. A., and Graham, S. A., 1994, Late Oligocene–early Miocene unroofing in the Chinese Tian Shan: An early effect of the India-Asia collision: *Geology*, v. 22, p. 487–490.
- Hodges, K. V., Hames, W. E., Olszewski, W. J., Burchfiel, B. C., Royden, L. H., and Chen, Z., 1994, Thermobarometric and $^{40}\text{Ar}/^{39}\text{Ar}$ geochronologic constraints on Eo-Himalayan metamorphism in the Dinggye area, southern Tibet: *Contributions to Mineralogy and Petrology*, v. 117, p. 151–163.
- Honegger, K., Dietrich, V., Frank, W., Gansser, A., Thoni, M., and Trommsdorff, V., 1982, Magmatism and metamorphism in the Ladakh Himalayas (the Indus-Tsangpo suture zone): *Earth and Planetary Science Letters*, v. 60, p. 253–292.
- Jin, Y., McNutt, M. K., and Zhu, Y.-S., 1996, Mapping the descent of Indian and Eurasian plates beneath the Tibetan Plateau from gravity anomalies: *Journal of Geophysical Research*, v. 101, p. 11275–11290.
- Kidd, W. S. F., Pan Yun, Chang Chengfa, Coward, M. P., Dewey, J. F., Gansser, A., Molnar, P., Shackleton, R. M., and Sun, Y., 1988, Geologic mapping of the 1985 Chinese-British (Xizang-Qinghai) Geotraverse route: *Royal Society of London Philosophical Transactions*, ser. A, v. 327, p. 287–305.
- Kong, X., Yin, A., and Harrison, T. M., 1997, Evaluating the role of preexisting weaknesses and topographic distribution in the Indo-Asian collision by use of a thin-shell numerical model: *Geology*, v. 25, p. 527–230.
- Le Fort, P., 1981, Manaslu, leucogranite: A collision signature of the Himalaya. A model for its genesis and its emplacement: *Journal of Geophysical Research*, v. 86, p. 10545–10648.
- Le Fort, P., 1996, Evolution of the Himalaya, *in* Yin, A., and Harrison, T. M., eds., *The tectonics of Asia*: Cambridge University Press, New York, p. 95–106.
- Leloup, H. P., Lacassin, R., Tapponnier, P., Schärer, U., Zhong Dalai, Liu Xiaohan, Zhang Laingshang, Ji Shaocheng, and Phan Trong Trinh, 1995, The Ailao Shan–Red River shear zone (Yunnan China) Tertiary transform boundary of Indochina: *Tectonophysics*, v. 251, p. 3–84.
- Le Pichon, X., Fournier, M., and Jolivet, L., 1992, Kinematics, topography, shortening, and extrusion in the India-Eurasia collision: *Tectonics*, v. 11, p. 1085–1098.
- Liu, Z. Q., compiler, 1988, *Geologic map of the Qinghai-Xizang Plateau*: Beijing, Chengdu Institute of Geology and Mineral Resources, Chinese Academy of Geological Sciences, Geological Publishing House, scale, 1:5 000 000.
- Lovera, O. M., Richter, F. M., and Harrison, T. M., 1989, $^{40}\text{Ar}/^{39}\text{Ar}$ geothermometry for slowly cooled samples having a distribution of diffusion domain sizes: *Journal of Geophysical Research*, v. 94, p. 17917–17935.
- Lovera, O. M., Grove, M., Harrison, T. M. and Mahon, K. I., 1997, Systematic analysis of K-feldspar $^{40}\text{Ar}/^{39}\text{Ar}$ step-heating experiments I: Significance of activation energy determinations: *Geochimica et Cosmochimica Acta*, v. 61, p. 3171–3192.
- Lyon-Caen, H., and Molnar, P., 1985, Gravity anomalies, flexure of the Indian plate, and the structure, support and evolution of the Himalaya and Ganga basin: *Tectonics*, v. 4, p. 513–538.
- Macfarlane, A. M., 1995, An evaluation of the inverted metamorphic gradient at Langtang National Park, central Nepal Himalaya: *Journal of Metamorphic Geology*, v. 13, p. 595–612.
- Makovsky, Y., Klemperer, S. L., Huang Liyan, and Lu Deyuan, 1996, Structural elements of the southern Tethyan Himalaya crust from wide-angle seismic data: *Tectonics*, v. 15, p. 997–1005.
- Matte, Ph., Tapponnier, P., Arnaud, N., Bourjot, L., Avouac, J. P., Vidal, Ph., Liu Qing, Pan Yusheng, and Wang Yi, 1996, Tectonics of western Tibet, between the Tarim and the Indus: *Earth Planetary Science Letters*, v. 142, p. 311–330.
- McDougall, I., and Harrison, T. M., 1988, *Geochronology and thermochronology by the $^{40}\text{Ar}/^{39}\text{Ar}$ method*: New York, Oxford University Press, 212 p.
- Miller, C., Schuster, R., Klötzli, U., Frank, W., and Purtscheller, F., 1999, Post-collisional potassic and ultrapotassic magmatism in SW Tibet: Geochemical and Sr-Nd-Pb-O isotopic constraints for mantle source characteristics and petrogenesis: *Journal of Petrology*, v. 40, p. 1399–1424.
- Mitra, G., 1994, Strain variation in thrust sheets across the Sevier fold-and-thrust belt (Idaho-Utah-Wyoming): Implications for section restoration and wedge taper evolution: *Journal of Structural Geology*, v. 16, p. 585–602.
- Molnar, P., and England, P., 1990, Temperatures, heat flux, and frictional stress near major thrust faults: *Journal of Geophysical Research*, v. 95, p. 4833–4856.
- Molnar, P., and Tapponnier, P., 1975, Tertiary tectonics of Asia: Effects of a continental collision: *Science*, v. 189, p. 419–426.
- Murphy, M. A., Yin, A., Kapp, P. A., Harrison, T. M., Ryerson, F. J., Chen Zhengle, and Wang Xiao-Feng, 1997, Miocene evolution of the Kailas thrust and Gurla Mandhata detachment fault, NW Tibet: Implications for slip history of the Karakoram fault: *Geological Society of America Abstracts with Programs*, v. 29, p. 143.
- Nelson, K. D., Zhao, W. J., Brown, L. D., Kuo, J., Che, J. K., Liu, X. W., Klemperer, S. L., Makovsky, Y., Meissner, R., Mechie, J., Kind, R., Wenzel, F., Ni, J., Nabelek, J., Chen, L. S.,

- Tan, H. D., Wei, W. B., Jones, A. G., Booker, J., Unsworth, M., Kidd, W. S. F., Hauck, M., Alsdorf, D., Ross, A., Cogan, M., Wu, C. D., Sandvol, E., and Edwards, M., 1996, Partial molten middle crust beneath southern Tibet: Synthesis of Project INDEPTH results: *Science*, v. 274, p. 1684–1687.
- Northrup, C. J., Royden, L. H., and Burchfiel, B. C., 1995, Motion of the Pacific plate relative to Eurasia and its potential relation to Cenozoic extension along the eastern margin of Eurasia: *Geology*, v. 23, p. 719–722.
- Owens, T. J., and Zandt, G., 1997, Implications of crustal property variations for models of Tibetan Plateau evolution: *Nature*, v. 387, p. 37–43.
- Pan, Y., 1993, Unroofing history and structural evolution of the southern Lhasa terrane, Tibetan Plateau: Implications for the continental collision between India and Asia [Ph.D. thesis]: Albany, State University of New York, 395 p.
- Patriat, P., and Achache, J., 1984, India-Asia collision chronology has implications for crustal shortening and driving mechanism of plates: *Nature*, v. 311, p. 615–621.
- Pecher, A., 1991, The contact between the Higher Himalaya Crystallines and the Tibetan Sedimentary Series: Miocene large-scale dextral shearing: *Tectonics*, v. 10, p. 587–598.
- Peltzer, G., and Tapponnier, P., 1988, Formation and evolution of strike-slip faults, rifts, and basins during the India-Asia collision: An experimental approach: *Journal of Geophysical Research*, v. 93, p. 15085–15117.
- Pognante, U., 1993, Different *P-T-t* paths and leucogranite occurrences along the High Himalayan Crystallines: Implications for subduction and collision along the northern Indian margin: *Geodinamica Acta*, v. 6, p. 5–17.
- Powell, C. M., and Conaghan, P. J., 1973, Plate tectonics and the Himalayas: *Earth and Planetary Science Letters*, v. 20, p. 1–12.
- Quidelleur, X., Grove, M., Lovera, O. M., Harrison, T. M., Yin, A., and Ryerson, F. J., 1997, Thermal evolution and slip history of the Renbu-Zedong thrust, southeastern Tibet: *Journal of Geophysical Research*, v. 102, p. 2659–2679.
- Ratschbacher, L., Frisch, W., Chen Chengsheng, and Pan Guitan, 1992, Deformation and motion along the southern margin of the Lhasa block (Tibet) prior to and during the India-Asia collision: *Geodynamics*, v. 16, p. 21–54.
- Ratschbacher, L., Frisch, W., Liu, G., and Chen, C. C., 1994, Distributed deformation in southern and western Tibet during and after the India-Asia collision: *Journal of Geophysical Research*, v. 99, p. 19917–19945.
- Royden, L. H., Burchfiel, B. C., King, R. W., Wang, E., Chen Zhiliang, Shen Feng, and Liu Yuping, 1997, Surface deformation and lower crustal flow in eastern Tibet: *Science*, v. 276, p. 788–790.
- Rumelhart, P. E., Yin, A., Butler, R., Richards, D., Wang Xiao-Feng, and Zhou Xian-Qiang, 1997, Oligocene initiation of deformation of northern Tibet, evidence from the Tarim basin, northwestern China: *Geological Society of America Abstracts with Programs*, v. 29, no. 6, p. A143.
- Ryerson, F. J., Yin, A., Harrison, T. M., and Murphy, M., 1995, The Gangdese and Renbu Zedong thrust systems: Westward extension to Mt. Kailas: *Geological Society of America Abstracts with Programs*, v. 27, no. 5, p. A335.
- Schärer, U., and Allègre, C. J., 1984, U-Pb geochronology of the Gangdese (Transhimalaya) plutonism in the Lhasa-Xigaze region, Tibet: *Earth and Planetary Science Letters*, v. 63, p. 423–432.
- Schärer, U., Xu, R. H., and Allègre, C. J., 1986, U-(Th)-Pb systematics and ages of Himalayan leucogranites, south Tibet: *Earth and Planetary Science Letters*, v. 77, p. 35–48.
- Schelling, D., 1992, The tectonostratigraphy and structure of the eastern Nepal Himalaya: *Tectonics*, v. 11, p. 851–862.
- Searle, M. P., 1996a, Cooling history, erosion, exhumation, and kinematics of the Himalaya-Karakoram-Tibet orogenic belt, in Yin, A., and Harrison, T. M., eds., *The tectonics of Asia*: New York, Cambridge University Press, p. 110–148.
- Searle, M. P., 1996b, Geologic evidence against large-scale pre-Holocene offsets along the Karakoram fault: Implications for limited extrusion of the Tibetan Plateau: *Tectonics*, v. 15, p. 171–186.
- Searle, M. P., Windley, B. F., Coward, M. P., Cooper, D. J. W., Rex, A. J., Rex, D., Tingdong, L., Xuchang, X., Jan, M. Q., Thakur, V., and Kumar, S., 1987, The closing of Tethys and the tectonics of the Himalaya: *Geological Society of America Bulletin*, v. 98, p. 678–701.
- Searle, M. P., Parrish, R. R., Hodges, K. V., Hurford, A., Ayres, M. W., and Whitehouse, M. J., 1997a, Shisha Pangma leucogranite, south Tibetan Himalaya: Field relations, geochemistry, age, origin, and emplacement: *Journal of Geology*, v. 105, p. 295–317.
- Searle, M., Corfield, R. I., Stephenson, B., and McMarron, J., 1997b, Structure of the North Indian continental margin in the Ladakh-Zaskar Himalayas: Implications for the timing of obduction of the Spontang ophiolite, India-Asia collision and deformation events in the Himalaya: *Geological Magazine*, v. 134, p. 297–316.
- Şengör, A. M. C., and Natal'in, B. A., 1996, Paleotectonics of Asia: Fragments of a synthesis, in Yin, A., and Harrison, T. M., eds., *The tectonics of Asia*: New York, Cambridge University Press, p. 486–640.
- Song, T., and Wang, X., 1993, Structural styles and stratigraphic patterns of syndepositional faults in a contractional setting: Example from Quaidam basin, northwestern China: *American Association of Petroleum Geologists Bulletin*, v. 77, p. 102–117.
- Srivastava, P., and Mitra, G., 1994, Thrust geometries and deep structure of the outer and lesser Himalaya, Kumaon and Garhwal (India): Implications for evolution of the Himalayan fold and thrust belt: *Tectonics*, v. 13, p. 89–109.
- Tapponnier, P., and Molnar, P., 1977, Active faulting and tectonics in China: *Journal of Geophysical Research*, v. 82, p. 2905–2929.
- Tapponnier, P., Peltzer, G., Le Dain, A. Y., Armijo, R., and Cobbold, P., 1982, Propagating extrusion tectonics in Asia: New insight from simple experiments with plastin: *Geology*, v. 10, p. 1339–1384.
- TBGMR (Tibetan Bureau of Geology and Mineral Resources), 1982, *Geology of the Xizang Autonomous Region*, 707 p.
- Thakur, V. C., and Sharma, K. K., 1983, *Geology of Indus suture zone of Ladakh, Dehra Dun, India*: Wadia Institute of Himalayan Geology, 204 p.
- Treloar, P. J., Rex, D. C., Guise, P. C., Coward, M. P., Searle, M. P., Windley, B. F., Petterson, M. G., Jan, M. Q., and Luff, I. W., 1989, K-Ar and Ar-Ar geochronology of the Himalayan collision in NW Pakistan: Constraints on the timing of suturing, deformation, metamorphism and uplift: *Tectonics*, v. 8, p. 881–909.
- Turner, S., Hawkeworth, C., Liu, J., Roger, N., Kelley, S., and van Calsteren, P., 1993, Timing of Tibetan uplift constrained by analysis of volcanic rocks: *Nature*, v. 364, p. 50–54.
- Wang, E., and Burchfiel, B. C., 1997, Interpretation of Tertiary tectonics in right-lateral accommodation zone between the Ailao Shan shear zone and the eastern Himalayan syntaxis: *International Geology Review*, v. 39, p. 191–219.
- Wang, S., Li, Z., and Qiangba, X., 1983, *Geologic map (1:1 000 000) and geologic report of the Xigaze area*: Tibetan Bureau of Geology and Mineral Resources, 568 p.
- Wiedmann, J., and Durr, S. B., 1995, First ammonites from the middle to Upper Cretaceous Xigaze Group, south Tibet and their significance: *Newsletters on Stratigraphy*, v. 32, p. 17–26.
- Willett, S. D., and Beaumont, C., 1994, Subduction of Asian lithospheric mantle beneath Tibet inferred from models of continental collision: *Nature*, v. 369, p. 642–645.
- Ye, C. H., and Huang, R. J., 1990, Tertiary stratigraphy of the Tarim Basin, in Zhou Z., and Chen, P., *Stratigraphy of the Tarim basin*: Beijing, Science Press, p. 308–363.
- Yin, A., Harrison, T. M., Ryerson, F. J., Chen, W. J., Kidd, W. S. F., and Copeland, P., 1994, Tertiary structural evolution of the Gangdese thrust system in southeastern Tibet: *Journal of Geophysical Research*, v. 99, p. 18175–18201.
- Yin, A., Harrison, T. M., Murphy, M. A., Ryerson, F. J., Chen, Z., Wang, X., and Zhou, X., 1996, How do we recognize sutures in ancient orogenic belts? Lessons learned from the Indus-Tsangpo “suture”: *Geological Society of America Abstracts with Programs*, v. 28, no. 7, p. A113.
- Yin, A., Nie, S., Craig, P., Harrison, T. M., Ryerson, F. J., Qian, X., and Yang, G., 1998, Late Tertiary tectonic evolution of the southern Chinese Tian Shan: *Tectonics*, v. 17, p. 1–27.
- Yu Zheng-Xing and Zhen An-Zhu, 1979, *Geologic map of the Lhasa region at a scale of 1:1 000 000*: Beijing, Geologic Publishing House.
- Zhao, W. L., and Morgan, W. J., 1985, Uplift of the Tibetan Plateau: *Tectonics*, v. 4, p. 359–369.
- Zhao Wenjin, Nelson, K. D., and Project INDEPTH, 1993, Project INDEPTH, deep seismic reflection evidence for continental underthrusting beneath southern Tibet: *Nature*, v. 366, p. 557–559.

MANUSCRIPT RECEIVED BY THE SOCIETY MARCH 3, 1998

REVISED MANUSCRIPT RECEIVED NOVEMBER 11, 1998

MANUSCRIPT ACCEPTED DECEMBER 17, 1998